Geosci. Model Dev. Discuss., 6, 521–584, 2013
www.geosci-model-dev-discuss.net/6/521/2013/
doi:10.5194/gmdd-6-521-2013

Geoscientific
Model Development
Discussions

Four-dimensional evaluation of regional air quality models

E. Solazzo[1], R. Bianconi[2], G. Pirovano[3], M. D. Moran[4], R. Vautard[5], C. Hogrefe[6], V. Matthias[7], P. Grossi[2], K. W. Appel[6], B. Bessagnet[9], J. Brandt[8], C. Chemel[12,13], J. H. Christensen[8], R. Forkel[16], X. V. Francis[13], A. Hansen[8], S. McKeen[17], U. Nopmongcol[14], M. Prank[11], K. N. Sartelet[10], A. Segers[15], J. D. Silver[8], G. Yarwood[14], J. Werhahn[16], J. Zhang[4], S. T. Rao[6], and S. Galmarini[1]

[1] Institute for Environment and Sustainability, Joint Research Centre, European Commission, ISPRA, Italy
[2] Enviroware srl, Concorezzo (MB), Italy
[3] Ricerca sul Sistema Energetico (RSE SpA), Milano, Italy
[4] Air Quality Research Division, Science and Technology Branch, Environment Canada, Toronto, Canada
[5] Laboratoire des Sciences du Climate et de l'Environnement, IPSL Laboratoire CEA/CNRS/UVSQ, Orme des Merisier, 91191 Gif/Yvette Cedex, France
[6] Atmospheric Modelling and Analysis Division, Environmental Protection Agency, NC, USA
[7] Institute of Coastal Research, Helmholtz-Zentrum Geesthacht, Geeshacht, Germany
[8] Department of Environmental Science, Aarhus University, Frederiksborgvej 399, 4000 Roskilde, Denmark
[9] Ineris, Parc Technologique Halatte, France

[10]CEREA, Joint Laboratory Ecole des Ponts ParisTech/EDF R & D,
Université Paris-Est, France
[11]Finnish Meteorological Institute, Helsinki, Finland
[12]National Centre for Atmospheric Science (NCAS), University of Hertfordshire, Hatfield, UK
[13]Centre for Atmospheric & Instrumentation Research (CAIR), University of Hertfordshire,
Hatfield, UK
[14]ENVIRON International Corporation, 773 San Marin Drive, Suite 2115, Novato,
CA 94998, USA
[15]Netherlands Organisation for Applied Scientific Research (TNO), Utrecht, The Netherlands
[16]Karlsruhe Institute of Technology, IMK-IFU, Garmisch-Partenkirchen, Germany
[17]CIRES/University of Colorado, and NOAA/ESRL/CSD, 325 Broadway, Boulder, CO, USA

Received: 27 November 2012 – Accepted: 7 January 2013 – Published: 24 January 2013

Correspondence to: E. Solazzo (efisio.solazzo@jrc.ec.europa.eu)

Published by Copernicus Publications on behalf of the European Geosciences Union.

Abstract

The evaluation of regional air quality models is a challenging task, not only for the intrinsic complexity of the topic but also in view of the difficulties in finding sufficiently abundant, harmonized and time/space-well-distributed measurement data. This study, conducted in the framework of AQMEII (Air Quality Model Evaluation International Initiative), evaluates 4-D model predictions obtained from 15 modelling groups and relating to the air quality of the full year of 2006 over the North American and European continents. The modelled variables are ozone, CO, wind speed and direction, temperature, and relative humidity. Model evaluation is supported by the high quality in-flight measurements collected by instrumented commercial aircrafts in the context of the MOZAIC programme. The models are evaluated at five selected domains positioned around major airports, four in North America (Portland, Philadelphia, Atlanta, Dallas) and one in Europe (Frankfurt). Due to the extraordinary scale of the exercise (number of models and variables, spatial and temporal extent), this study is primarily aimed at illustrating the potential for using MOZAIC data for regional-scale evaluation and the capabilities of models to simulate concentration and meteorological fields in the vertical rather than just at the ground. We apply various approaches, metrics, and methods to analyze this complex dataset. Results of the investigation indicate that, while the observed meteorological fields are modelled with some success, modelling CO in and above the boundary layer remains a challenge and modelling ozone also has room for significant improvement. We note, however, that the high sensitivity of models to height, season, location, and metric makes the results rather difficult to interpret and to generalize. With this work, though, we set the stage for future process-oriented and in-depth diagnostic analyses.

1 Introduction

The development of policies designed to control and reduce air pollution requires an accurate knowledge about the sensitivity of atmospheric concentration levels to changes in anthropogenic emissions. This sensitivity is modulated by a number of factors, including atmospheric conditions and their variability, the state of the land surface, which modulates deposition and biogenic emissions, imported pollutant concentrations, and the primary emissions that produce a chemical environment in which secondary air pollutants develop. All of these factors influence and are influenced by the distribution of pollutants in the vertical direction. Therefore, to accurately predict sensitivity to emissions, complex air quality (AQ) models being used for policy development must be able to correctly predict the four-dimensional (in the horizontal, vertical, and time) pollutant distribution in the troposphere.

Precise simulation of tropospheric fields is not only crucial from the perspective of emission control, but also to test the capability of models to capture the vertical distribution of pollutants, the exchanges between the boundary layer and the free troposphere, as well as the horizontal fluxes to and from continental domains (Jonson et al., 2010; Gilge et al., 2010; Brunner et al., 2005). Since pollutants such as ozone and particulate matter (PM) are known to be harmful to human health and to ecosystems, it is important that models reliably predict their transport from source to receptor regions in both the short and long range, as well as vertical exchange between the stratosphere, free troposphere, and planetary boundary layer. At the same time, in order to rule out the possibility of compensating errors, it is important to assess the capability of models to simulate processes and constituents other than atmospheric chemistry and aerosols, in particular the meteorological fields (wind, humidity, temperature) that drive the transport and dispersion of pollutants, as errors in these meteorological fields are inherited by AQ models, thereby producing errors in model-predicted pollutant concentrations. This is particularly the case for long-lived species, whose concentrations are determined by history of air parcels over long time periods during which meteorological errors may accumulate (e.g. Brunner et al., 2003; Blond and Vautard, 2004).

The evaluation of regional AQ systems is a long standing research topic both for model development and application and for model evaluation and assessment (e.g. Van Loon et al., 2007; Vautard et al., 2009, 2012; Solazzo et al., 2012a,b). The majority of model evaluation studies are typically focused on the assessment of model performance with respect to surface measurements, since their primary goal is to simulate the fate of pollutants to which humans, and the biosphere as a whole, are exposed. Consequently, performances of AQ models in the troposphere (from ground to well above the boundary layer) have not been evaluated as often, both in terms of pollutants such as ozone and CO and relevant meteorological fields. Although some specific studies carried out in field campaigns (e.g. Cros et al., 2004, Drobinski et al., 2007; Yu et al., 2007, 2010; Wei et al., 2011) or case studies (e.g. Emeis et al., 2011; Matthias et al., 2012) do exist, full three- and four-dimensional evaluation and model inter-comparisons over long time periods are missing. Recently, a large community effort was put together within the Air Quality Modelling Evaluation International Initiative (AQMEII) that, among several objectives, intended to evaluate regional AQ models in a 4-dimensional (4-D) sense (Rao and Galmarini, 2011).

Examples of 4-D ensemble model evaluation do exist for global chemical transport models. Stevenson et al. (2006) analysed 26 global model runs and estimates based on ozonesonde profiles for the year 2000 and suggested that the primary sources of ozone in the troposphere are chemical production and influx from the stratosphere (this latter was estimated as being about a tenth of the production term), and that removal is determined by chemical transformation and dry deposition. Furthermore, the authors showed that the ensemble mean of model results for ozone typically ranges within one standard deviation of the measurements over the entire depth of the troposphere. However, several significant discrepancies were detected, depending on location and season. A further example of ensemble modeling of tropospheric ozone is reported by Jonson et al. (2010), who compared the ensemble mean from 12 models against ozonesonde profiles in the framework of HTAP for the year 2001. The ensemble mean bias of models was found to be smaller in winter and autumn, with day-to-day variability greatly different from one model to another, and generally models were found to perform better at locations closer to major sources than in remote locations. The authors attributed such behaviour of the models to the difficulties to resolve plumes at remote stations due to the coarse resolution of global models. Most recently Zyryanov et al. (2012) conducted a comparative 3-D analysis of six regional AQ models over Europe using MOZAIC observations, focusing on ozone during the summer months of 2008. The authors found that a large model-to-model variability exists in the upper troposphere. Although a definite justification for such variability could not be identified, the authors pointed out a few aspects that can be held, at least partially, responsible: the model transport schemes and grid resolution (both in the horizontal and in the vertical), the different treatment of the top boundary conditions, and the way that vertical velocity is computed (diagnostically or as output of the meteorological model).

There are a number of individual case studies where individual regional models are compared to 3-dimensional concentrations, in particular during extensive measurement campaigns. However, AQMEII is the first case study where systematic ensemble model results can be compared with observations collected over two continents by means of commercial aircraft flights connecting the two. This is the objective of the present study, which complements previous studies made in the context of the AQMEII project, where model evaluation was done against large sets of ground-based data for ozone (Solazzo et al., 2012a), particulate matter (Solazzo et al., 2012b), and meteorological fields (Vautard et al., 2012). As presented in Rao et al. (2011), the first goal of the analysis is the operational evaluation of models, trying therefore to identify the discrepancies between models and measurements and to produce hypotheses that should then be investigated in detail as part of the subsequent diagnostic evaluation. Operational evaluation is in fact the first step toward a comprehensive model performance assessment as described by Dennis et al. (2010), which was the conceptual framework for model evaluation adopted by AQMEII.

This study demonstrates the existence, usability, and usefulness of observational information in the vertical that can be combined to produce relevant information for model development, evaluation, and improvement. The exploitation of upper air information produced by different sources over a regional domain allows a thorough verification of model fundamentals that is seldom achieved, not because they are assumed to be unimportant but because of the difficulties in finding harmonized measurement data (or finding them collected over long periods). This is the first study of its kind. Although it is not intended to be an in-depth diagnostic analysis, it illustrates the potential for using MOZAIC data for regional-scale evaluation, introduces various approaches, metrics, and methods to analyze this complex dataset, and sets the stage for future work. Particular attention is paid to ozone in this study due to its importance in air quality and climate and because a complementary model evaluation for ground-level ozone is available (Solazzo et al., 2012a). Thus, ozone is used to illustrate how 4-D datasets can be effectively used to assess seasonal and boundary condition errors.

2 Processing of four-dimensional observational data in the context of AQMEII

In this study, we make use of the observational data for the year 2006 gathered in the context of the MOZAIC programme (Measurements of Ozone, water vapor, carbon monoxide and nitrogen oxides by Airbus In-service aircraft; http://mozaic.aero.obs-mip.fr/web/) and made available in the ENSEMBLE system (Galmarini et al., 2004, 2012) in the context of the AQMEII inter-comparison and model evaluation activity. In addition to the MOZAIC data, ozonesonde measurements are also used for further comparison in special cases.

The MOZAIC project started in 1993 as a joint effort of European scientists, aircraft manufacturers and airlines for better understanding of the natural and human-induced variability of the chemical composition of the atmosphere. The vast collection of data includes a large number of vertical profiles measured at several airports worldwide during the landing and take-off phases. Collected data include meteorological variables (wind speed and direction, temperature, relative humidity) and chemical species (CO, NO, NO_x, NO_y, O_3). The sampling rate of data collection is of 4 s, corresponding to approximately 50–100 m in the vertical. The limit of detection is rather low (2 ppbv for ozone) with error of 2 %, thus making the MOZAIC dataset very accurate. Details of MOZAIC data acquisition can be found in Marenco et al. (1998); Thouret et al. (1998).

Permission to access to the MOZAIC dataset for the reference year of 2006 was granted to the AQMEII community, allowing the analysis of over 2000 vertical profiles measured by instrumented commercial aircraft landing and taking-off from 12 selected airports in North America (Portland, Vancouver, Atlanta, Dallas, Charlotte, Boston, Chicago, Montreal, New York, Philadelphia, Toronto, Washington, DC) and three in Europe (Frankfurt, Munich and Vienna). These profiles contain the following species and meteorological fields: ozone, carbon monoxide (CO), temperature (T), relative humidity (RH), wind speed (WS) and direction (WD). Modelling groups were requested to deliver data of the same species. Observation and model outputs have been paired in the web shared ENSEMBLE system, as detailed hereafter.

The strategy adopted within AQMEII for the comparison with the MOZAIC dataset consisted of plotting all the aircraft trajectories up to the altitude of approximately 13 km at all available airports for 2006 in the two continents. Domains were then identified at each airport location that contained all the trajectories over the year. This was particularly useful in the case, for example, of the Northeast US where trajectories of aircrafts landing in Washington, DC passed over New York airports too. Similarly in Europe, all the trajectories relating to Vienna also passed over Munich and Frankfurt. After the identification of the MOZAIC trajectory domains, 13 vertical levels above ground were identified (at 0, 100, 250, 500, 750, 1000, 2000, 3000, 4000, 5000, 6000, 7500, 8500 m) which are relevant to the analysis of the model results. Extraction has been made taking the value at closest model level for each observation level. To simplify the data request and extraction to modelers, four areas were identified in North America (NA) and one in Europe (EU), grouping the trajectory projections of several airports together (see Fig. 3 in Galmarini et al., 2012 and detail therein). All modelers were then asked to deliver the model data corresponding to the 3-D grids enclosing the MOZAIC trajectories and at the identified altitudes with a common horizontal grid resolution for the whole period of 2006 with one hour time resolution. The 4-D data volumes were subsequently delivered to European Commission's Joint Research Centre at Ispra (Italy) by each modeling group and included in the ENSEMBLE system, a web-interfaced data hub allowing modeling an observed data to be harmonized and paired in time and space so to facilitate the model evaluation. Once a specific airport, date, and flight were selected, the ENSEMBLE system automatically extracted the model data from the domain volume and coupled them with the MOZAIC profiles in x,y,z and t. Since measurements and model results are stored in ENSEMBLE at the same heights, the trajectory analysis module in ENSEMBLE works by looping through the measurement points along each three-dimensional trajectory. ENSEMBLE extracts the model value at the grid node longitude and latitude coordinates that are closest to those of the measurement, so that the model value is the best available representation of the measurement.

For all the airports included in this study, data gathered during take-offs and landings mostly occurred between the early-to-mid-afternoon (landing in NA) and the mid-to-late afternoon (take-offs in NA) (local time), more frequently in summer than in winter. Table 1 gives the list of airports within each simulation domain and the number of MOZAIC flights to each airport during 2006. To simplify the analysis, for each of the five areas (four in NA and one in EU), the airport with the largest number of flights was selected and used for analysis. Therefore, Portland and Philadelphia were selected to represent the west and east coasts of NA, respectively, and Dallas and Atlanta represented two other areas of NA. Frankfurt (with over 1200 hourly flights) has the best yearly coverage and represents the central EU area. The location of the airports and flight areas are shown in Fig. 1.

2.1 Ozonesonde measurements

Ozonesonde data were extracted from the WMO World Ozone and Ultraviolet Radiation Data Centre in Toronto (Canada). These measurements report vertical profiles of ozone partial pressure on vertical pressure levels and these data too are available on the ENSEMBLE system paired with modelled outputs of a number of variables.

3 Participating models

The participating models and modelling groups are reported in Table 2. In total, four to five (depending on the variable) modelling groups delivered data to compare against the MOZAIC profiles for NA, whereas outputs from eight to nine modelling groups were available for EU. For NA, four different AQ models were employed:

- AURAMS (Gong et al., 2006; Smyth et al., 2009)
- CAMx (ENVIRON, 2010)
- CMAQ (Byun and Schere, 2006)
- DEHM (Brandt et al., 2012)

The above AQ models were driven by meteorological inputs generated by the GEM, WRF, COSMO-CLM (CCLM), and MM5 meteorological models. In particular, two sets of CMAQ results are available, which used meteorological inputs from CCLM and WRF, respectively. This pair of results can thus provide some insights into the impact of the meteorological module used on the vertical variability of AQ variables.

The eight AQ models providing outputs for EU were:

- DEHM;
- SILAM (Sofiev et al., 2006);
- CHIMERE (Bessagnet et al., 2004);
- LOTOS-EUROS (Schaap et al., 2008);
- CMAQ;

- CAMx;

- WRF/Chem (Grell et al., 2005).

- Polyphemus (Sartelet et al., 2012)

These AQ models were driven by meteorological inputs generated by the WRF, CCLM, MM5, and ECMWF meteorological models. Compared to the NA case, an additional meteorological driver for the EU case is the ECMWF model, driving the SILAM and LOTOS-EUROS models. Similar to the NA case, two sets of CMAQ results were again available based on meteorological inputs from the CCLM and WRF meteorological models. An interesting and original outcome of this study is provided by comparing the performance of the same AQ model run over two different continents, also in light of the several numerical schemes and algorithms adopted by the models for simulating the advection and vertical transport (discussed in Sect. 3.1). The performance of three AQ models – CAMx, CMAQ, and DEHM – can be examined in this light. Two modelling groups (one based in Europe and the other in North America) applied the WRF-WRF/Chem model over Europe with identical setup except that one simulation included feedback between meteorology and atmospheric chemistry (referred to as WRF/Chem1) and the other did not (WRF/Chem2).

The emissions and chemical boundary conditions used by the various AQMEII groups are also summarised in Table 2. AQMEII provided a set of reference time-varying gridded emissions (referred to as the “standard” emissions) for each continent, focusing on the evaluation of the AQ and meteorological models. These inventories have been extensively discussed in other AQMEII publications (Pouliot et al., 2012; Solazzo et al., 2012a,b). The standard emissions were used by the vast majority of the participating AQMEII groups (Table 2), but even if “standard” emissions were used, there were still a number of degrees of freedom, e.g. fire emissions or biogenic emissions, which were chosen by each group independently. Model results generated with other emissions inventories have also been submitted, however, which provides a useful comparison in interpreting the results of model-estimated ozone and CO concentrations.

AQMEII also made available a set of time-dependent chemical concentrations at the lateral boundaries of the EU and NA domains, referred to as the "standard" boundary conditions, which were extracted from the Global and regional Earth-system Monitoring using Satellite and in-situ data (GEMS) re-analysis product provided by European Centre for Medium-range Weather Forecast (see Schere et al., 2012 for more details). These standard boundary conditions were used by most but not all participating AQMEII groups. Other boundary conditions for ozone used by several AQMEII modeling groups were based on satellite measurements assimilated within the Integrated Forecast System (IFS). Models were driven by different meteorological simulations, which were described and evaluated in Vautard et al. (2012). Details are given in Table 2.

3.1 Participating models and settings

3.1.1 WRF-CMAQ

The CMAQ model configurations run by the US EPA and the University of Herthfordshire were similar for NA and EU, with both simulations utilizing version 4.7.1 (Foley et al., 2010) of the model. The NA simulation used 34-vertical layers and 12-km horizontal grid spacing covering the CONUS, southern Canada and northern Mexico, while the EU simulation used 34 vertical layers and 18-km horizontal grid spacing covering most of EU. For the NA domain, the height of the first layer was at roughly 40 m, the model top was at 50 mb, and there were 11 layers below 1 km. Other model options employed that were common to both simulations include the CB05 chemical mechanism with chlorine chemistry extensions, the AERO5 aerosol module (Carlton et al., 2010), and the Asymmetric Convective Model 2 (ACM2) vertical mixing scheme (Pleim, 2007a,b).

3.1.2 ECMWF-SILAM

The SILAM model uses a transport algorithm based on the non-diffusive Eulerian advection scheme of Galperin (1999, 2000) and the adaptive vertical diffusion algorithm of Sofiev (2002). The use of sub-grid variables in these schemes allows the model to run with thick vertical layers. A more detailed description can be found in Sofiev et al. (2008). SILAM includes a meteorological pre-processor for diagnosing the basic features of the boundary layer and the free troposphere (e.g. diffusivities) from the meteorological fields provided by meteorological models (Sofiev et al., 2010). Only horizontal wind components are taken from the meteorological input and the vertical component is computed from continuity equation. SILAM runs in terrain-following height coordinates and for the AQMEII runs the model vertical consisted of 9 layers up to ~ 10 km. The model values were linearly interpolated to the requested heights.

3.1.3 MM5-DEHM

The Danish Eulerian Hemispheric Model (DEHM) (Christensen, 1997; Frohn et al., 2002; Brandt et al., 2012) is a 3-D long-range atmospheric chemistry-transport model with a horizontal domain covering the Northern Hemisphere with a 150 km × 150 km resolution. In this study, the model was set up with two two-way nested domains simultaneously – one covering EU and one covering NA, both with 50 km × 50 km resolution. The vertical grid is defined using the σ-coordinate system, with 29 vertical layers extending up to a height of 100 hPa. The horizontal advection is solved numerically using the higher-order Accurate Space Derivatives scheme, applied in combination with a Forester filter. The vertical advection, as well as the dispersion sub-models, is solved using a finite elements scheme for the spatial discretisation. For the temporal integration of the dispersion, the method is applied and the temporal integration of the three dimensional advection is carried out using a Taylor series expansion to third order. The 3-D wind fields are applied from the MM5 model, corrected in DEHM to ensure mass conservation. DEHM also includes a module for diagnostically calculating the vertical wind. For ozone, the initial and boundary conditions (lateral and top) are based on ozonesonde measurements, interpolated to global monthly 3-D values with a resolution of 4° × 5° (Logan, 1999). A thorough description of DEHM and model setup for AQMEII is given in Brandt et al. (2012).

3.1.4 MM5-CHIMERE

The CHIMERE model (Bessagnet et al., 2004; Schmidt et al., 2001) is run over Europe at a 0.25° resolution and uses a 9-layer vertical resolution expressed in a hybrid-sigma pressure coordinate system between surface and the 500 hPa pressure level. The first near-surface layer height was 20 m. It is therefore a lower-troposphere model. All meteorological fields are interpolated from driver meteorology (MM5), but vertical velocity is then recalculated from mass balance. Turbulence in the boundary layer is represented using a diffusivity coefficient. The formulation uses K-diffusion following the parameterization of Troen and Mahrt (1986) without the counter-gradient term. The second-order Van Leer scheme is used for the horizontal transport, and horizontal diffusion is neglected. Top boundary conditions are issued from the GEMS re-analysis at 3-h resolution and interpolated in three dimensions. The depth of the boundary layer is taken directly from MM5. Full model documentation is available at http://www.lmd.polytechnique.fr/chimere/.

3.1.5 ECMWF-LOTOS-EUROS

The LOTOS-EUROS model (Schaap et al., 2008) simulates concentrations over Europe at a regular grid of 0.5° × 0.25° degrees (about 25 km). In the vertical, the model is defined on four layers: a 25 m surface layer, the boundary layer, and 2 residual layers with a top at 3.5 km a.s.l. (or higher in mountainous areas); the model could therefore be regarded as a boundary layer model. The height of the boundary layer, as well as the other meteorological input, is taken from ECMWF meteorological fields (short range forecasts over 0–12 h at 3-h resolution). Advection of tracers is implemented in all three dimensions following Walcek (2000), where vertical mass fluxes are derived from the mass balance. Vertical mixing is mainly determined by the growth of the second model layer following the rise of the boundary layer during the day, which leads to mixing of concentrations from the residual to the lower layer. An additional vertical mixing is implemented following standard K-diffusion (Louis, 1979). In horizontal direction, no explicit diffusivity is added apart from the numerical diffusion implied by the advection on a discrete grid. Lateral and top boundary conditions are taken from the standard ECMWF-GEMS re-analysis data available for the AQMEII project (Schere et al., 2012).

3.1.6 MM5-Polyphemus

The Polyphemus air-quality modeling platform is used with the Polair3-D Eulerian chemistry transport model (Sartelet et al., 2012). Over Europe, the horizontal resolution is 0.25°. Polyphemus uses terrain-following height coordinates with 9 vertical layers from 20 m to 9 km for the AQMEII simulation. The reactive-transport equations are solved using operator splitting (sequence: advection, diffusion, chemistry and aerosol). The advection scheme is a direct space-time third-order scheme with a Koren flux-limiter. Diffusion and chemistry are solved with a second-order Rosenbrock method. The vertical eddy-diffusion coefficient is parameterized following Louis (1979), except in the unstable convective boundary layer where the coefficients are calculated using the parameterization of Troen et Mahrt (1986). The horizontal diffusion coefficient is set constant and equal to 10 000 $m^2 s^{-1}$. In the AQMEII simulation, meteorological fields are interpolated from MM5, except for the eddy-diffusion coefficient and the vertical velocity, which is deduced from the continuity equation. Lateral and top boundary conditions are the default AQMEII boundary conditions provided by ECMWF-GEMS.

3.1.7 GEM-AURAMS

The AURAMS model was run for AQMEII on a North American domain using a secant polar-stereographic map projection true at 60° N and 45-km horizontal grid spacing.

Title Page
Abstract
Introduction
Conclusions
References
Tables
Figures
◀◀
▶▶
◀
▶
Back
Close
Full Screen / Esc
Printer-friendly Version
Interactive Discussion

In the vertical, 29 levels were used with a terrain-following modified-Gal-Chen vertical coordinate and relatively thin layers near the surface (the first five levels were located at 0, 14, 55, 120, and 196 m) increasing monotonically in thickness to a model top at ∼ 22 km. Horizontal and vertical advection were both calculated using a semi-Lagrangian advection scheme (e.g. Pudykiewicz et al., 1997) with wind components provided by the GEM meteorological model (Côté et al., 1998a,b; Mailhot et al., 2006). The vertical diffusion operator was solved using an implicit first-order Laasonen scheme, where the vertical eddy-diffusion coefficient was parameterized in GEM using a turbulence kinetic energy scheme (Benoit et al., 1989; Belair et al., 1999). Horizontal diffusion was neglected. Unfortunately, model output was only saved for the first 20 levels, so that vertical profiles are only available for the AURAMS model up to ∼ 5 km.

3.1.8 WRF-WRF/Chem

The only model with atmospheric chemistry coupled online with the meteorology applied within this study was the community model WRF/Chem. The two instances of WRF/Chem applied for Europe here differ only by one aspect: one included feedback of the direct and indirect aerosol radiative effect to meteorology, and one did not. Both simulations were set up with a horizontal grid spacing of 22.5 km, 36 layers in the vertical direction, and identical physics and chemistry options as described by Forkel et al. (2012). Gas-phase/aerosol chemistry and non-hydrostatic physics within WRF/Chem are tightly coupled, with 5th-order horizontal, 3rd-order vertical, and a 3rd-order Runge–Kutta time integration scheme (Skamarock et al., 2008). YSU boundary layer physics (Hong et al., 2006) is used for vertical mixing within the PBL. Boundary conditions for all species are from the default WRF/Chem configuration, which were designed to be representative for clean, mid-latitude Pacific ocean conditions. In spite of major differences in simulated solar radiation for cloudy conditions (Forkel et al., 2012) only small differences between the two model versions were found, since simulated temperature, humidity, and wind were nudged to the driving global analysis above the PBL for the simulations discussed here.

3.1.9 Cosmo-CLM-CMAQ

At HZG Institute, the CMAQ model is set up on a 24 × 24 km^2 gird and 30 vertical layers for both continents. Eleven of the 30 layers are below 1 km, with the lowest layer top in 36 m. CMAQ4.6 (Matthias et al., 2010; Aulinger et al., 2011) was used for the EU domain and CMAQ 4.7.1 for NA (the same run by the other participants). Horizontal and vertical advection schemes in CMAQ use a modification of the piecewise parabolic method (PPM, Colella and Woodward, 1984). At each grid cell, from the horizontal advection a vertical velocity component is derived that satisfies the continuity equation using the driving meteorology model's density. In CMAQ 4.7.1 this scheme was further modified by adjusting the vertical velocities by the ratio of upwind fluxes to PPM calculated fluxes. Vertical diffusion is based on the asymmetric convective model (ACM, Pleim and Chang, 1992). In both CMAQ 4.6 and 4.7.1 its version 2 (ACM2, Pleim, 2007, 2007a) is implemented. The minimum value for the eddy diffusivity depends on the land use in the individual grid cells. It varies between 0.5 m^2 s^{-1} in grid cells with no urban areas to 2 m^2 s^{-1} in grid cells that contain only urban area. Zero flux boundary conditions are used at the horizontal borders and at the top of the domain.

3.1.10 WRF/MM5-CAMx

CAMx simulations for NA and EUROPE used model version 5.21 (ENVIRON, 2010) and the CB05 chemical mechanism (Yarwood et al., 2005). The European domain had 0.125° by 0.25° latitude-longitude resolution and 23 vertical layers that followed WRF pressure levels between the surface and 100 mb. The NA domain had 12 km horizontal resolution and 26 layers that followed MM5 pressure levels between the surface and 50 mb. The boundary conditions and emissions provided by AQMEII were used with the exception that biogenic emissions for Europe were estimated using MEGAN

(Guenther et al., 2006). The CAMx vertical transport scheme is described by Emery et al. (2011) with vertical advection solved by a backward-Euler (time) hybrid centred/upstream (space) scheme and vertical diffusion solved using K-theory.

4 Model performance in the troposphere

The results discussed in this section are based on model-to-model and model-to-observation comparisons for 2006 for the airports in each of the MOZAIC domains with the largest number of available data (flights) (i.e. Portland, Philadelphia, Dallas, Atlanta, and Frankfurt).

4.1 Mean vertical profiles

We present comparison of seasonal averaged mean profiles of ozone and annual averaged mean profiles of CO, temperature, RH and WS against observational MOZAIC data. Profiles are shown in Fig. 2. The data used are the vertical profiles (ascending and descending) spatially averaged over the areas around the airports. Observations are the symbols in grey.

It can be firstly observed how all models show very similar mean profiles of wind (above the PBL) and temperature (from ground to last level), in agreement with the observed ones, although these fields are generated by meteorological models run by different groups. This most likely descends from the influence of nudging technique applied to the input analysis fields. One interesting aspect of the WS profiles is that the positive bias of the MM5-DEHM, that increases with the altitude (all sites). This is probably due to the coarser resolution of this model with respect to the others. Differently, RH profiles agree with observations within the first ∼2 km, but significantly diverge above that height at all sites. It should be noted, however, that being the relative humidity derived from the specific humidity and the temperature, in regions where water vapour mixing ratio is very low (that is, in the diverging zone), even small differences in the temperature fields can give rise to relevant differences in RH. The RH peaks clearly at 1000 m at all airports, although with different magnitudes. With the exception of Dallas, the peak is generally well captured by the models.

Concerning the chemical species of CO and ozone, the mean profiles of Fig. 2 tend show the model sensitivity to the boundary conditions (BCs): indeed, looking at NA sites, models sharing GEMS boundary conditions are clearly closer each other than DEHM, that is driven by different large scale fields (model sensitivity to BCs is further discussed in Sect. 6). The seasonal ozone measurements show the lowest levels in winter (all airports) and the typical maximum in spring and summer. The mean ozone concentration increases with altitude in the first kilometres of the troposphere, as near the ground depletion by deposition and titration reduce the ozone availability (e.g. Chevalier et al., 2007). The strong effect of surface processes on ozone is also revealed by the strong gradient in the first 2000 m of the troposphere, ranging on average between 10 to 20 ppb km^{-1} at all sites. Modelled ozone in winter is typically biased low at all locations, with the exception of DEHM (both NA and EU). The CCLM-CMAQ, MM5-CAMx, and SILAM in EU are biased high above ~6000 m throughout the year, probably due to the upper BCs being too close to the modelled height. PBL ozone is generally overestimated in summer (NA only), whilst is closer to the observed values in fall, especially for Frankfurt (detailed further in Sect. 6). Mean profiles of observed CO show a steep decrease of concentration in the first 2000 m, with an average gradient ranging between ~ −24 ppb km^{-1} (Dallas and Philadelphia) and −37 ppb km^{-1} (Atlanta), whilst is of −57 ppb km^{-1} at Frankfurt. Between 2000 m and 8000 m the decrease in CO concentration is sensibly milder, with a gentle gradient of ~5–6 ppb km^{-1} at all airports. Averaged profiles of modelled CO show that ground level concentrations can differ up to a factor of 2, although differences are milder above the PBL (~1000 m), but still significant as discussed in detail with the aid of Taylor diagram in Sect. 4.2.4 (the large range of the horizontal scale has the effect of grouping the profiles, thus deceptively reducing the bias). A possible reason for such a difference might be related to the horizontal resolution of the AQ model. Indeed, as shown in Table 2, the

DEHM model, that adopted the coarsest resolution, simulated the lowest concentrations, whereas CAMx and CMAQ provided the highest ones (e.g. Brunner et al., 2003). Such behaviour is confirmed by ozone profiles, mainly in winter periods, where models showing highest CO concentrations, simulated the lowest O_3 ground level concentrations, probably due a stronger titration effect. Another reason could be related to the boundary conditions, as discussed later in Sect. 6.

4.2 Operational statistics and variability

In this section, annual average statistics are presented with Taylor diagrams (Taylor, 2001), which simultaneously show error, standard deviation and Pearson Correlation Coefficient (PCC) for wind speed, relative humidity, ozone, and CO. In a Taylor plot, the observed field is represented by a point at a distance from the origin along the abscissa that is equal to the variance. All other points on the plot area represent values for the simulated fields and are positioned such that the variance of the modelled fields is the radial distance from the origin, the correlation coefficient of the two fields is the cosine of the azimuthal angle (desired value: 1), and the RMSE is the distance to the observed point (desired value: 0). In practical terms, the closer a model point is to an observed point, the better the model performance.

Although seasonal variations are thought to be important, to synthesise the discussion we present annually averaged statistics (Figs. 3 to 6). At any given height, the number of paired observation-model data is the same as the number of MOZAIC flights for all of 2006 reported in Table 2. Because flight paths differ between ascents and descents and can also vary due to meteorological conditions, the horizontal spatial location of the various measurements for a given altitude will also vary, and computing a temporal average across all data points also implies computing a spatial average. The spatial coverage of the virtual "horizontal plane" containing the individual flight trajectories over which the spatial averaging is calculated depends on the height. In fact, while the $z = 0$ level has the spatial coverage of a point (having the airport's coordinates), that of the $z = 8500$ m level is much larger, containing all the trajectories (ascending and descending) to and from the airport. This aspect has an influence on the spread of the data, as we shall discuss next.

Performance for temperature is considered to be satisfactory for all models, at all domains for, at least, the first 5000 m (PCC in excess of 0.90 and bias ≤ 0.01 K). For this reason, analysis for temperature is not shown.

Coefficients of variation – defined as the ratio between the standard deviation and the average of the annual distribution at any height – have also been calculated for the aforementioned fields (for the sake of synthesis are only shown for Frankfurt in Fig. 7).

4.2.1 Wind Speed

A common feature that can be inferred at all of the airports is that all models show an overestimation of the wind speed in the first 100 m, together with poor correlation with the observed values. A similar, though less pronounced, positive bias can be observed also at 500 and 1000 m. These features are similar for all models at all sites, thus stating that state of art meteorological models are still weak in reproducing wind speed inside the PBL, the most relevant portion of the atmosphere in relation to air quality processes, as already found by Vautard et al. (2012) for the case of surface measurements. The poor model performance in the first 100 m at all sites is also confirmed by the analysis of the coefficients of variation, with modelled values well below the observations. Looking at the Taylor diagrams of Figure 3 and also at the coefficients of variation (not shown), an interesting feature is the clustering of model performance depending on altitude rather than on models, thus indicating that correct reproduction of wind speeds within the PBL, and near the surface, is a common difficulty for all models. There may be several reasons for this deficiency. First of all, unlike upper-air winds as measured by rawinsondes, surface winds are not used for producing reanalyses. Thus even with a strong nudging of wind field to reanalyses a lower model skill is expected for surface winds as compared to upper-air winds. Second, near-surface winds are sensitive to several driving factors besides the synoptic circulation, such as land cover, processes driving the exchange of energy at surface, for which global and regional models are known to largely differ from one another (see, e.g. de Noblet-Ducoudré et al., 2012; Stegehuis et al., 2012).

As we move away from the surface, the performance improves. The height of 500 m is a clear separator for the performance of all models at all sites, and more markedly near the two coasts of NA, at Portland and Philadelphia, where starting from 500 m up to the top, PCC, error and variability improve consistently. In general, the best performance by all models are observed for $z \geq 3000$ m with PCC > 0.8 at all NA sites and, with the exception of WRF/Chem (PCC ~ 0.65 at $z = 3000$ m), also at Frankfurt.

4.2.2 Wind direction

Although of pivotal importance for the transport of the polluted air masses, evaluation of the modelled wind direction is often overlooked. In this section we summarise the results of evaluating the AQ models of Table 2 using wind direction data from ground to 8500 m. To simplify the analysis we have binned the frequency counts of the occurrences of wind direction angle with 45 degree interval. Results in terms of normalised bias (modelled minus observed count, and divided by the observed count) are discussed next for each airport. For the sake of brevity, no supporting graphs are shown. In general, a few points are worth making:

- The bias in the PBL for the Frankfurt airport is smaller and decreases faster with height with respect to the NA airports;

- For NA airports, the two instances of WRF do not always provide the same counts at all heights and at all locations. These two fields were derived from the same underlying WRF simulation. Therefore, the differences seen in this analysis were introduced when the two modeling groups independently interpolated these fields to the common horizontal and vertical analysis grid defined for the MOZAIC analysis under AQMEII and transferred these processed fields to ENSEMBLE. Thus, these differences highlight the difficulties in attributing differences in model performance to differences in model options, in particular for quantities with significant horizontal and vertical gradients such as wind direction;

- At NA airports, in general there is a large bias within the PBL which is most pronounced on the west coast (Portland);
- The bias pattern in the PBL of the EU airport is common to all tested models (eight available for wind direction) and the instances of MM5 (forcing the CAMx, Polyphemous and Chimere models) are identical.

Portland. From the ground to 500 m, WRF-CMAQ and GEM show similar biases: positive for north-west and negative for south-east (about 100 %). The other models are biased low in the eastern sector. From $z = 500$ m the bias becomes larger and all models show a clear tendency to overestimate the occurrences of westerly and easterly winds, for example, WRF-CMAQ simulated more than three times as many occurrences of westerly winds compared to observations. At about PBL height ($z = 1000$ m) and up to 2500 m, the bias is reduced and models reproduced the frequency distribution of observed wind direction well. From 3000 m up to the top, the observed direction of the wind is predominantly from the south-west and models generally capture this feature.

Philadelphia. The bias of all models from the ground to 250 m is relatively small. Both WRF and GEM exhibit a positive bias for the south-west to west sectors. At 500 m, the two WRF instances show twice as many occurrences of winds from the north as present in the MOZAIC observations. From the PBL height up to 5000 m the observed wind direction is largely from the south-east and all of the models agree well with the observations except that both WRF simulations exhibit a positive bias for the frequency of occurrence of southerly winds at 4000 m.

Atlanta. In the first 250 m all models are biased high in the west and north-west directions (50 %). GEM and WRF-CAMx are biased low in the north direction (–100 %). At 500 m WRF-CAMx still shows a low bias in the north direction which WRF-CMAQ is unbiased, and all models are biased high in the north-eastern and south-western directions (from 50 to 100 %). At PBL height most of the bias is restricted to the south-west and the north-east directions, and reduces to values close to zero as the height increases.

Dallas. The east-west positive bias detected for all of the models in the first 250 m turns clockwise at 500 m, directed in the north-west direction. Whilst remaining biased high in the north-west direction, GEM and WRF-CAMx models acquire a south-western bias component (about 70 %) at $z = 1000$ m. The bias progressively decreases from 2000 m up.

Frankfurt. All of the models share similar bias patterns. At ground, the tendency is to underestimate the occurrences of northerly winds (all models) and to overestimate the westerly components (with different magnitude by all models). The ECMWF driving the LOTOS-EUROS model also overestimates the east component at ground and at 100 m, which might be explained from this model using average values over the boundary layer for the second model layer. At this height, the bias is still high towards south west. As the height increases, the bias reduces progressively.

4.2.3 Relative humidity

In contrast to wind speed, models show less spread with height in reproducing relative humidity and show a more marked dependence on airport. The temporal variability is underestimated by all models, as shown by the sigma ratio values, ranging between 0.8 and 1 at all airports, with the exception of Portland. Also the analysis of the coefficients of variation reveals that there is a slight tendency to under predict the observed variability, more markedly detected for $z > 6000$ m. Model performance are (as in the case of the wind speed) in general grouped by height, although with a few exception (as the WRF/Chem at Frankfurt, Fig. 4e). The best performance takes place between 500 and 1000 m, while it tends to deteriorate with height. As already mentioned, this could be due to the water vapour mixing ratio being very small aloft, making relative humidity computation less and less reliable at higher altitudes.

4.2.4 CO

Modelled CO show the largest range of modelled/observed standard deviations detected in this study, at all heights, for all airports. Correlation is typically below 0.6 at all sites and all heights, with very few exceptions. Errors are also large at all altitudes and mainly in the first 250 m. All models fail in reproducing the temporal variability of CO concentrations. This might be related to the influence of local sources close to the airport whose temporal modulation is not captured by the models. Analysis of the coefficient of variations demonstrates how the variability is highly overestimated in the PBL at all NA sites (up to a factor of two at Dallas, Atlanta, and Philadelphia). Performance improves slightly with height, giving the best scores in the range of altitudes between 2000 and 4000 m. This can be due to a stronger dependence to large-scale transport of boundary conditions combined with the fact that winds are nudged at these altitudes. In the PBL, CO concentration result from a more complex mix between transport and emission in the lower troposphere.

It should be also mentioned that for long lived species such as CO the error of the meteorological fields also puts limits on the performance, thus inaccuracies in modelled wind speed, direction, etc. might accumulate over time contributing to worsening the model scores for CO (e.g. Brunner et al., 2003). To test these explanations for CO, we calculated the correlations between the errors (at the same height) of the modelled CO concentration with those of wind speed. Results of this analysis (not shown) proved that indeed there are instances (e.g. AURMAS and DEHM at Philadelphia for $z = 1000$ m; CAMx at Dallas for $z = 4000$ m) when the two fields are significantly and positively correlated (up to values of ~ 0.35). However, it was not possible to unveil a pattern of general validity, as correlations are generally poor and take place at different heights for different airports and models.

4.2.5 Ozone

Ozone is a topical species and one of the most extensively evaluated in the proximity of surface. Evaluation of the regional models employed in this analysis against surface level measurements presented by Solazzo et al. (2012) has revealed an overall good model performance over both the continental domains of NA and EU (but superior for NA). The yearly averaged Taylor diagrams of Fig. 6 shows that indeed the skills of the models are better near the ground ($z \leq 1000$ m) than aloft, with the exception of Portland, where models perform better above the PBL, possibly due to the vicinity of the edge of the computational domain, therefore being more sensitive to the influence of BCs. Also the bias in the WD detected in Sect. 4.2.2 at this airport might have an influence. Ozone skills are clustered by height and by modelling group, rather than simply by AQ model. The two instances of CMAQ (driven by WRF and CCLM), for example, do not produce similar results at any of the NA airports (they used the same BCs and emissions). By contrast, the two AQ models driven by WRF (CMAQ and CAMx) display rather similar results. These results might point to the weight of the meteorological driver for ozone as well as to the importance of diverse modelling approaches. This is not entirely confirmed by the Taylor plots for Frankfurt (where WRF is the driver for WRF/Chem and CMAQ) though, as the results are primarily grouped by AQ models (note that all of these models use the same BCs). In fact the two instances of CMAQ in this case are rather close to each other (but it should be noted that the modelling group that ran WRF-CMAQ for EU was not the same of that of NA).

Model performance in the PBL on the east coast of the US (Philadelphia) are higher than for the west coast (Portland), with higher correlation (exceeding 0.8 at 500 m), and are also satisfactory at Dallas and Atlanta. This may be due to a more accentuate dependence emission rather than on BCs leading to a better variability away from the west border of the NA continent. The variability and the coefficient of variations are underestimated at Portland but in good agreement with the measured values at the other NA airports (with the exception of the DEHM model, underestimating the coefficient of variations at all locations, possibly due to the use of RCP emissions in the NA domain in DEHM). At Frankfurt, we can notice the best agreement (PCC, variability and error) between 500 m and 1000 m (WRF-CMAQ and Chimere are among the best models in this range), and WRF/Chem performing the worst in terms of variability. The latter may be attributed to the fact that at this height, the simulated values are already influenced to some extent by the applied (standard WRF/Chem) boundary conditions, which are too low particularly in spring and summer at this range of height and also above (see Fig. 2). The variability and errors above 3000 m and up to 8500 m reveals some model deficiencies. From the mean seasonal profiles of Fig. 2 models underestimate ozone between 3000 and 6000, but they overestimate it aloft (see Frankfurt for example) (though not systematically at all locations and all seasons by all models). This could be due to model under-prediction of the exchange between the upper troposphere and the lower stratosphere and/or to diffusive model errors related to coarse vertical gridding. Brunner et al. (2003), by contrast, report a tendency of global chemistry models to overestimating ozone mixing ratios in the NA continental-scale domain between 5.5–8 km throughout the year (results based on the period 1995–1998). We should notice, however, that whilst those results were averaged over all the NA continent, here we are comparing regional scale models at much finer scales, and the different behaviour could be attributed simply to the different resolution of the two approaches.

5 Altitudinal correlations

Aiming at investigating whether errors result from common sources at surface and upper air, a correlation analysis is applied in this section. If different processes cause errors aloft and errors near the ground, one would expect little or no correlation between time series of errors calculated at different levels. For example, if errors near the surface result primarily from the treatment of PBL processes, deposition, or emissions, these errors should not be correlated with the errors further aloft. Conversely, in the case of “large-scale errors” one expects that under- or over-estimations are simultaneous at different altitudes, and therefore correlated. The investigation is carried out for ozone, CO, RH and WS. Figure 8 reports how the fractional difference (FD) at ground is correlated with that at height $z > 0$ for all investigated airports. FD is defined as:

$$\mathrm{FD} = \frac{\mathrm{Mod} - \mathrm{Obs}}{0.5\,(\mathrm{Mod} + \mathrm{Obs})} \tag{1}$$

where FD, Mod and Obs are N-length vectors denoting the modelled and the observed field value, respectively. Here N is the number of hourly flights available for the period being analysed (for example, for the full year the values of Table 1 are used). The correlations are calculated between the N-length FD vector at ground with the N-length FD vector at other levels.

The analysis of the FD correlation profiles clearly shows that for all variables (some exceptions for CO) and airports the FD is contained in the PBL and that ground and aloft biases are poorly correlated. The correlation drops down very quickly with height for both wind speed and relative humidity. Particularly, wind and relative humidity present the strongest vertical gradient as well as the most homogenous behaviour among the different models. The obtained results hence suggest that the proper simulation of PBL wind speed and relative humidity is strongly influenced by processes taking place within the PBL itself (the only exceptions are the two instances of WRF/WRF-Chem at Frankfurt). In contrast, FD correlation profiles for CO exhibit the most scattered behaviour. They vary aloft between 0.1–0.2 and 0.4–0.6, the latter results generally produced by MM5-DEHM for which the hypothesis of large scale error might explain the correlation between bias at ground and at height. It is worth noting that DEHM results reflect the strong vertical mixing shown by the mean vertical profiles (Fig. 2). The relevant differences shown by CO results, compared to the clustered performance of wind and humidity suggest that turbulent mixing plays a relevant role in determining the vertical profiles of air pollutants. Ozone FD correlation is more homogeneous than CO among the different models, also showing to be more correlated with height than wind and relative humidity. This supports the hypothesis that the vertical ozone profile is the result of an interplay between an ozone reservoir in the upper troposphere and ground level concentrations (Zhang and Rao, 1999; Godowitch et al., 2011), thus increasing the correlation between ozone values at different heights.

These results point out the need for a more quantitative evaluation of vertical mixing, for example by establishing some indicators that could be compared to observed quantities.

6 Altitudinal error: the case of ozone

The seasonal error associated with the model's capability in predicting ozone mixing ratios in the vertical is investigated for all airports and models. The error is expressed in terms of fractional absolute difference (FAD), defined as:

$$\mathrm{FAD} = \frac{|\mathrm{Mod} - \mathrm{Obs}|}{0.5(\mathrm{Mod} + \mathrm{Obs})} \quad (2)$$

(the elements in Eq. 2 have the same meaning of Eq. 1). Results are presented for the winter months of January and February (Fig. 9) and for the summer months of June, July, and August (Fig. 10) in terms of cumulative FAD (that is, the sum of model errors at each height). The bars in Figs. 9 and 10 reflect the accumulated error of all models at each altitude. Since the number of models is about twice as high for EU than for NA (9 vs. 5), one would expect the cumulative FAD for EU to be about double that for NA. In the winter, however, the cumulative FAD for Frankfurt at the surface as well as above is larger than expected compared to the NA airports. At the ground this is partially due to the large errors of the SILAM, CAMx and LOTOS-EUROS models. With increasing height, the errors of CAMx and LOTOS-EUROS drop, while SILAM's remains high. In the summer, by contrast, cumulative FAD at Frankfurt is about double of that of Philadelphia and Dallas but of the same magnitude of that of Portland and Atlanta, where all of the models exhibit higher errors than at Philadelphia and Dallas (the AURAMS model has the highest error). At Portland and Atlanta airports most models showed a clear overestimation of both CO yearly mean concentrations as well as ozone summer concentrations. The marked decrease of FAD with height shown by Fig. 9 confirms that model discrepancies are mainly related to surface processes. Particularly, errors could descend from an overestimation of emissions in the surrounding area giving rise to an excess of CO and ozone production by primary precursors. As for ozone, the underestimation of deposition processes could also be a source of influence (see also Sect. 6.1 for further details on ozone bias in the surface layer). Other features of relevance:

- The error of the WRF-CMAQ model at the ground of Philadelphia in winter is larger than the other instance of CMAQ driven by CCLM due to a higher tritration effect; Fig. 2 also shows that WRF-CMAQ exhibits the strongest CO concentration, suggesting that differences between the two CMAQ runs can be driven by the adopted vertical diffusion scheme.
- The CCLM-CMAQ model has error increasing with height at Portland in winter, negligible at ground and of significance from 500 m up. This suggests that the model is able to capture the surface layer equilibrium between NO_x and ozone, driven by titration, differently from other models missing it; it is also worth noting that aloft CCLM-CMAQ performances are very close the other models pointing out low level processes are not strongly influenced by ozone aloft;
- The error above 5000 m at NA airports is the smallest detected. At this height only the error of DEHM model preserve the same magnitude of the error below. The high error at 8500 m for EU is due to models whose top level is close to that height, as for example the SILAM model.

6.1 Bias due to boundary conditions

In the previous section we presented the altitudinal error of ozone. In this section we present a further application of 4-D model evaluation by providing comparison between the lateral boundary conditions for ozone used by the AQ models and the vertical profiles of ozone measured onboard MOZAIC aircrafts. We show the analysis for NA only, as the vicinity of airports to the edges of the modelled domain allows testing the influence of the BCs more effectively. Details about the preparation of the BCs in AQMEII are provided by Schere et al. (2012).

Hourly profiles averaged over the months of January and August are used for comparison, from the Vancouver and Portland (west coast) and Philadelphia (east coast) airports. Vertical profiles of:

- monthly averaged BCs for ozone adopted by the AQ models;
- monthly averaged AQ model profiles of ozone over the selected airports;
- monthly averaged MOZAIC measurements of ozone at the selected airports with the observed standard deviation at each altitude.
- For the month of August 2006 we make also use of ozonesonde data collected at locations close to the Philadelphia airport, as specified in the text (shown in Fig. 11).

Results of the comparison are reported in Figs. 11–16.

The GEMS BCs were adopted by the WRF-CMAQ, CCLM-CMAQ, and CAMx models (Table 2); AURAMS group used its own BCs, while ozone BCs for DEHM are extracted from climatology and satellite measurements and applied to the model's outer domain which encompasses the whole north hemisphere. The concentration profiles at the DEHM's inner domains (one centred in NA and one in EU), which reflect the dynamics of the hemispheric domain, have been taken here for comparison (grid point where the profiles were extracted is shown in Fig. 11).

During wintertime, the absence of strong photochemical activity amplifies the influence of boundary conditions. It can be observed that aloft ($z > 2000$ m), the ozone monthly profiles at both sites overlap to a large extent the corresponding boundary profiles (Figs. 13–15). The only exception is DEHM showing an increasing difference along height with respect to its boundary profile. As a consequence, also the bias with respect to the observed MOZAIC profiles reflects exactly the error shown by the boundary conditions. Within the PBL, the computed profiles show a sharper gradient than aloft due to the titration effect, but the ozone concentrations clearly reflect the influence of boundary conditions acting as an offset to surface concentrations. This result confirms that during wintertime the mean bias in ground level concentration is mostly driven by large scale background concentrations. This is further demonstrated by the correlation analysis shown in Fig. 13, where the normalised bias of:

- the BCs with respect to the MOZAIC, and
- the modelled ozone concentration with respect to MOZAIC

are plotted. The regression analysis shows some high correlation coefficients (especially for AURAMS and WRF-CMAQ). When the data of the first levels close to the ground are removed, the correlation coefficients are even higher. This is not entirely surprising as Schere et al. (2012) found that the boundary concentration profile specification for ozone was very influential on AQMEII model results far into the interior of the model simulation domain. This was especially true for the winter months and for rural areas away from major emission sources. Systematic underestimates of tropospheric ozone by the global modeling system that was used to derive the boundary concentrations for AQMEII modeling caused the regional-scale models to often underestimate NA near surface ozone concentrations.

During the summer season models show a different behaviour. At Portland site (Fig. 14) all models underestimate the aloft observed concentration and once again the computed concentration at the airport site is partially influenced by the boundary contribution. Differently, within the PBL, all models overestimate the observed concentrations of about 20–25 ppb. The overestimation seems to be related to an overestimation of vertical mixing in the PBL. Indeed, modelled concentrations are close to the observed ones around 1500–2000 m, while at the surface the models are not able to replicate the sharp decreasing gradient taking place in the MOZAIC profile and confirmed by the measurements at ground level receptors. Such a gradient is usually due to the titration effect of NO_X surface emissions together with surface deposition, whose gradient is underestimated by the models. Although the aircrafts fly rapidly away from/to the airport the urban influences of the large urban area around the airport is expected to increase the ozone gradient in the lowest levels due to fast titration by NO. This effect is expected to vanish aloft (Chevalier et al., 2007). Concerning the influence of boundary concentrations, it can be noted that differences in the aloft boundary concentrations profiles are observed also in the modelled aloft values and in turn in ground level concentrations. This is not the case for DEHM, where, once again, vertical mixing seem playing the dominant role.

Also at Philadelphia site, models tend to slightly underestimate the aloft concentrations (Fig. 16), while overestimate the observed concentrations within the PBL. The models driven by GEMS boundary conditions and AURAMS, to a lesser extent, replicate very well the observed profile between 1500 and 4000 m, while DEHM overestimates it. It is worth noting that models driven by GEMS fields show relevant differences within the first 3000 m, though they all cluster around the corresponding boundary value in the upper layers. The spread among models is driven by photochemistry whose effect is stronger in Philadelphia than Portland, being the east coast subject to higher emission loads than the western areas (see e.g. Appel et al., 2012). Ground level concentrations produced by models driven by the same GEMS fields range between 45 and 65 ppb, suggesting that summer ozone concentrations in polluted area are mainly related to local production than large scale background concentrations. This result is confirmed by DEHM that exhibits the highest surface concentrations, although it was fed by the lowest boundary concentration values. For the Philadelphia domain, ozonesondes profiles for the month of August were available from two rural sites Fig. 16). Measurements at the site STN487 site were collected every day of August at 18:00 GMT (Greenwich Mean Time), while there are 12-hourly measurements from the STN420, collected at different hour of the day, between 04:00 UGT and 20:00 GMT.

The availability of these extra profiles in rural parts of the domain allows confirming what MOZAIC data already pointed out about the ozone background concentration at the site the influence of titration on modelled ozone profile within the PBL.

7 Summary and conclusions

This study is conducted in the framework of the AQMEII activity and presents evaluation of regional scale air quality models. The evaluation is supported by measurements gathered in the MOZAIC campaign. The amount of information we present is unprecedented. Fifteen modelling groups have delivered 3-D data of ozone, CO, wind field, relative humidity with hourly resolution for the full year of 2006 at selected areas around major airports in Europe and North America. All of these data have been paired with observations in the ENSEMBLE system and made ready for analysis. Although this study is not aimed at in-depth diagnostic analysis, it illustrates the potential for using MOZAIC data for regional-scale evaluation, it introduces various approaches, metrics, and methods to analyze this complex dataset, and it sets the stage for future work. Due to its importance, we have devoted deeper analysis to ozone. Based on the results of our investigations the following considerations could be drawn, although the high sensitivity of models to height, season, location, and metric which make the results rather difficult to interpret and to generalize.

- Analysis of variability through coefficients of variation shows that model performance increases with height for WS and decreases with height for RH and partially for ozone;
- modelled CO show the largest range of modelled/observed standard deviations detected in this study, at all heights, for all airports. Correlation is typically below 0.6 at all sites and all heights, with very few exceptions. Errors are also large at all altitudes and mainly in the first 250 m. All models fail in reproducing the temporal variability of CO concentrations. This might be related to the influence of local

sources close to the airport whose temporal modulation is not captured by the models. Performance improves slightly with height, giving the best scores in the range of altitudes between 2000 and 4000 m;

- the yearly averaged Taylor diagrams for ozone shows that the skills of the models are superior near the ground ($z \leq 1000$ m) than aloft. Model performance in the PBL on the east coast of the US (Philadelphia) are higher than for the west coast (Portland), with higher correlation (exceeding 0.8 at 500 m), and are also satisfactory at Dallas and Atlanta;

- results obtained by correlating the bias at the ground with that at heights for ozone and CO point out the need for more quantitative evaluation of vertical mixing, for example establishing some indicators that could be compared to observed quantities;

- a common feature that can be inferred at all of the airports is that all models show an overestimation of the wind speed in the first 100 m, together with poor correlation with the observed values. A similar, though less pronounced, positive bias can be observed also at 500 and 1000 m. These features are similar for all models at all sites, thus indicating a need for improvement of state-of-art meteorological models in reproducing wind speed inside the PBL, the most relevant portion of the atmosphere in relation to air quality processes. In general, the best performance by all models are observed for $z \geq 3000$ m with PCC > 0.8 at all NA sites and, with the exception of WRF/Chem (PCC ~ 0.65 at $z = 3000$ m), also at Frankfurt.

- Differently from wind speed, models show less spread with height in reproducing relative humidity and show a more marked dependence on location. The best performance takes place between 500 and 1000 m, while it tends to deteriorate with height. This could be due to the water vapour mixing ratio being very small aloft, making relative humidity computation less and less reliable at higher altitudes.

- Analysis of wind direction throughout the troposphere shows that model bias in the PBL for the Frankfurt airport is smaller and decreases faster with height with respect to the NA airports. Furthermore, at NA airports a large bias within the PBL is observed which is most pronounced on the west coast;

- analysis of the correlation profiles of bias at ground with the bias at heights shows that for all variables (some exceptions for CO) and airports the bias is contained in the PBL and that ground and aloft biases are un-correlated. The correlation drops down very quickly with height for both wind speed and relative humidity. The results hence suggest that the proper simulation of PBL wind speed and relative humidity is strongly influenced by processes taking place within the PBL itself (the only exceptions are the two instances of WRF/WRF-Chem at Frankfurt).

- Analysis of error induced by boundary conditions for ozone in the north American continent indicates that during wintertime the mean bias in ground level concentration is mostly driven by large scale background concentrations.

- Conversely, the same analysis conducted for August 2006 suggests that summer ozone concentrations in polluted area are mainly related to local production and surface removal processes than large scale background concentration; the comparison with MOZAIC profiles suggest that the former is probably overestimated while the latter is underpredicted.

Acknowledgements. The MOZAIC Data Centre and its contributing airlines provided North American and European aircraft takeoff and landing vertical profiles are kindly acknowledged. The WMO World Ozone and Ultraviolet Data Centre (WOUDC) and its data contributing agencies provided North American and European ozonesonde profiles. GY and UN acknowledge financial support from the Coordinating Research Council Atmospheric Impacts Committee (Project A-75) and the Electric Power Research Institute. The contribution of RSE SpA to this work has been partially financed by the Research Fund for the Italian Electrical System under the Contract Agreement between RSE SpA and the Italian Ministry of Economic Development (Decree of 19 March 2009).

Title Page
Abstract | Introduction
Conclusions | References
Tables | Figures
◀| |▶
◀ ▶
Back | Close
Full Screen / Esc
Printer-friendly Version
Interactive Discussion

Disclaimer. Although this work has been reviewed and approved for publication by the US Environmental Protection Agency, it does not reflect the views and policies of the agency.

References

Appel, W., Chemel, C., Roselle, S. J., Francis, X. V., Hu, R.-M., Sokhi, R. S., Rao, S. T., and Galmarini, S.: Examination of the Community Multiscale Air Quality (CMAQ) model performance for North America and Europe for the AQMEII project, Atmos. Environ., 53, 142–155, 2012.

Aulinger, A., Matthias, V., and Quante, M.: An approach to temporally disaggregate Benzo (a) pyrene emissions and their application to a 3-D Eulerian atmospheric chemistry transport model, Water Air Soil Poll., 216, 643–655, 2011.

Bélair, S., Mailhot, J., Strapp, J. W., and MacPherson, J. I.: An examination of local versus nonlocal aspects of a TKE-based boundary-layer scheme in clear convective conditions, J. Appl. Meteor., 38, 1499–1518, 1999.

Benoit, R., Côté, J., and Mailhot, J.: Inclusion of TKE boundary-layer parameterization in the Canadian regional finite-element model, Mon. Wea. Rev., 117, 1726–1750, 1989.

Bessagnet, B., Hodzic, A., Vautard, R., Beekmann, M., Cheinet, S., Honoré, C., Liousse, C., and Rouil, L.: Aerosol modeling with CHIMERE: preliminary evaluation at the continental scale, Atmos. Environ., 38, 2803–2817, 2004.

Bessagnet, B., Seigneur, C., and Menut, L.: Impact of dry deposition of semi-volatile organic compounds on secondary organic aerosols, Atmos. Environ., 44, 1781–1787, doi:10.1016/j.atmosenv.2010.01.027, 2010.

Blond, N. and Vautard, R.: Three-dimensional ozone analyses and their use for short-term ozone forecasts, J. Geophys. Res., 109, D17, doi:10.1029/2004JD004515, 2004.

Bond, T. C., Bhardwaj, E., Dong, R., Jogani, R., Jung, S., Roden, C., Streets, D. G., Fernandes, S., and Trautmann, N.: Historical emissions of black and organic carbon aerosol from energy-related combustion, 1850–2000, Glob. Biogeochem. Cy., 21, GB2018, doi:10.1029/2006GB002840, 2007.

Boynard, A., Beekmann, M., Foret, G., Ung, A., Szopa, S., Schmechtig, C., and Coman, A.: An ensemble assessment of regional ozone model uncertainty with an explicit error representation, Atmos. Environ., 45, 784–793, 2011.

Brandt, J., Silver, J. D., Frohn, L. M., Geels, C., Gross, A., Hansen, A. B., Hansen, K. M., Hedegaard, G. B., Skjøth, C. A., Villadsen, H., Zare, A., and Christensen, J. H.: An integrated model study for Europe and North America using the Danish Eulerian Hemispheric Model with focus on intercontinental transport, Atmos. Environ., 53, 156–176, 2012.

Brunner, D., Staehelin, J., Rogers, H. L., Köhler, M. O., Pyle, J. A., Hauglustaine, D., Jourdain, L., Berntsen, T. K., Gauss, M., Isaksen, I. S. A., Meijer, E., van Velthoven, P., Pitari, G., Mancini, E., Grewe, G., and Sausen, R.: An evaluation of the performance of chemistry transport models by comparison with research aircraft observations – Part 1: Concepts and overall model performance, Atmos. Chem. Phys., 3, 1609–1631, doi:10.5194/acp-3-1609-2003, 2003.

Brunner, D., Staehelin, J., Rogers, H. L., Köhler, M. O., Pyle, J. A., Hauglustaine, D. A., Jourdain, L., Berntsen, T. K., Gauss, M., Isaksen, I. S. A., Meijer, E., van Velthoven, P., Pitari, G., Mancini, E., Grewe, V., and Sausen, R.: An evaluation of the performance of chemistry transport models – Part 2: Detailed comparison with two selected campaigns, Atmos. Chem. Phys., 5, 107–129, doi:10.5194/acp-5-107-2005, 2005.

Byun, D. and Schere, K. L.: Review of the governing equations, computational algorithms, and other components of the models-3 Community Multiscale Air Quality (CMAQ) modeling system, Appl. Mech. Rev., 59, 51–77, 2006.

Carlton, A. G., Bhave, P. V., Napelenok, S. L., Edney, E. O., Sarwar, G., Pinder, R. W., Pouliot, G. A., Houyoux, M.: Model representation of secondary organic aerosol in CMAQv4.7, Environ. Sci. Technol., 44, 8553–8560, 2010.

Chevalier, A., Gheusi, F., Delmas, R., Ordóñez, C., Sarrat, C., Zbinden, R., Thouret, V., Athier, G., and Cousin, J.-M.: Influence of altitude on ozone levels and variability in the lower troposphere: a ground-based study for western Europe over the period 2001–2004, Atmos. Chem. Phys., 7, 4311–4326, doi:10.5194/acp-7-4311-2007, 2007.

Christensen, J. H.: The Danish Eulerian Hemispheric Model – a three-dimensional air pollution model used for the Arctic, Atmos. Environ., 31, 4169–4191, 1997.

Colella, P. and Woodward, P. R.: The Piecewise Parabolic Method (PPM) for gas-dynamical simulations, J. Comput. Phys., 54, 174–201, 1984.

Corbett, J. J. and Fischbeck, P. S.: Emissions from ships, Science, 278,823–824, 1997.

Côté, J., Desmarais, J.-G., Gravel, S., Méthot, A., Patoine, A., Roch, M., and Staniforth, A.: The operational CMC/MRB Global Environmental Multiscale (GEM) model – Part I: Design considerations and formulation, Mon. Wea. Rev., 126, 1373–1395, 1998a.

Côté, J., Desmarais, J.-G., Gravel, S., Méthot, A., Patoine, A., Roch, M., and Staniforth, A.: The operational CMC/MRB Global Environmental Multiscale (GEM) model – Part II: Results, Mon. Wea. Rev., 126, 1397–1418, 1998b.

Cros, B., Durand, P., Frejafon, E., Kottmeier, C., Perros, P., Peuch, V.-H., Ponche, J.-L., Robin, D., Said, F., Toupance, G., and Wotham, H.: The ESCOMPTE program: an overview, Atmos. Res., 69, 241–279, 2004.

De Noblet-Ducoudré, N., Boissier, J.-P., Pitman, A., Bonan, G. B., Brovkin, V., Cruz, F., Delire, C., Gayler, V., van den Hurk, B., Lawrence, P. J., van der Mollen, M. K., Müller, C., Reick, C. H., Strengers, B. J., and Voldoire, A.: Determining robust impacts of land-use-induced land cover changes on surface climate over North America and Eurasia: results from the first set of LUCID experiments, J. Climate, 25, 3261–3281, 2012.

Dennis, R., Fox, T., Fuentes, M., Gilliland, A., Hanna, S., Hogrefe, C., Irwin, J., Rao, S. T., Scheffe, R., Schere, K., Steyn, D., and Venkatram, A.: A framework for evaluating regional-scale numerical photochemical modelling systems, Environ. Fluid Mech., 10, 471–489, doi:10.1007/s10652-009-9163-2, 2010.

Drobinski, P., Saïd, F., Ancellet, G., Arteta, J., Augustin, P., Bastin, S., Brut, A., Caccia, J. L., Campistron, B., Cautenet, S., Colette, A., Cros, B., Corsmeier, U., Coll, I., Dabas, A., Delbarre, H., Dufour, A., Durand, P., Guénard, V., Hasel, M., Kalthoff, N., Kottmeier, C., Lemonsu, A., Lohou, F., Masson, V., Menut, L., Moppert, C., Peuch, V. H., Puygrenier, V., Reitebuch, O., and Vautard, R.: Regional transport and dilution during high pollution episodes in southeastern France: summary of findings from the ESCOMPTE experiment. J. Geophys. Res., 112, D13105, doi:10.1029/2006JD007494, 2007.

Emeis, S., Forkel, R., Junkermann, W., Schäfer, K., Flentje, H., Gilge, S., Fricke, W., Wiegner, M., Freudenthaler, V., Groß, S., Ries, L., Meinhardt, F., Birmili, W., Münkel, C., Obleitner, F., and Suppan, P.: Measurement and simulation of the 16/17 April 2010 Eyjafjallajökull volcanic ash layer dispersion in the northern Alpine region, Atmos. Chem. Phys., 11, 2689–2701, doi:10.5194/acp-11-2689-2011, 2011.

Emery C. A., Tai, E., Yarwood, G., and Morris, R.: Investigation into approaches to reduce excessive vertical transport over complex terrain in a regional photochemical grid model, Atmos. Environ., 45, 7341–7351, doi:10.1016/j.atmosenv.2011.07.052, 2011.

ENVIRON: User's Guide to the Comprehensive Air Quality Model with Extensions (CAMx) version 5.20, available at: http://www.camx.com (last access: 9 November 2012), 2010.

Fischer, H., Lawrence, M., Gurk, Ch., Hoor, P., Lelieveld, J., Hegglin, M. I., Brunner, D., and Schiller, C.: Model simulations and aircraft measurements of vertical, seasonal and latitudinal O_3 and CO distributions over Europe, Atmos. Chem. Phys., 6, 339–348, doi:10.5194/acp-6-339-2006, 2006.

Foley, K. M., Roselle, S. J., Appel, K. W., Bhave, P. V., Pleim, J. E., Otte, T. L., Mathur, R., Sarwar, G., Young, J. O., Gilliam, R. C., Nolte, C. G., Kelly, J. T., Gilliland, A. B., and Bash, J. O.: Incremental testing of the Community Multiscale Air Quality (CMAQ) modeling system version 4.7, Geosci. Model Dev., 3, 205–226, doi:10.5194/gmd-3-205-2010, 2010.

Forester, C. K.: Higher order monotonic convective difference schemes, J. Comput. Phys., 23, 1–22, 1977.

Forkel, R., Werham, J., Hansen, A. B., McKeen, S., Peckam, S., Grell, G., and Suppan, P.: Effect of aerosol-radiation feedback on regional air quality – a case study with WRF/Chem, Atmos. Environ., 53, 202–211, 2012.

Frohn, L. M., Christensen, J. H., and Brandt, J.: Development of a high resolution nested air pollution model – the numerical approach, J. Comput. Phys., 179, 68–94, 2002.

Galmarini, S., Bianconi, R., Addis, R., Andronopoulos, S., Astrup, P., Bartzis, J. C., Bellasio, R., Buckley, R., Champion, H., Chino, M., D'Amours, R., Davakis, E., Eleveld, H., Glaab, H., Manning, A., Mikkelsen, T., Pechinger, U., Polreich, E., Prodanova, M., Slaper, H., Syrakov, D., Terada, H., and Van der Auwera, L.: Ensemble dispersion forecasting – Part II: Application and evaluation. Atmos. Environ., 38, 4619–4632, 2004.

Galmarini, S., Bianconi, R., Appel, W., Solazzo, E., Mosca, S., Grossi, P., Moran, M., Schere, K., and Rao, S. T.: ENSEMBLE and AMET: two systems and approaches to a harmonized, simplified and efficient facility for air quality models development and evaluation, Atmos. Environ., 53, 51–59, 2012.

Galperin, M. V.: Approaches for improving the numerical solution of the advection equation, in Large-Scale Computations in Air Pollution Modelling, edited by: Zlatev, Z., Brandt, J., Builtjes, P. J. H., Carmichael, G., Dimov, I., Dongarra, J., van Dop, H., Georgiev, K., Hass, H., and San Jose, R., Kluwer Acad., Dordrecht, Netherlands, 161–172, 1999.

Galperin, M. V.: The approaches to correct computation of airborne pollution advection, in: Problems of Ecological Monitoring and Ecosystem Modelling (in Russian), vol. 17, Gidrometeoizdat, St. Petersburg, Russia, 54–68, 2000.

Gazdag, J.: Numerical convective schemes based on accurate computation of space derivatives, J. Comput. Phys., 13, 100–113, 1973.

Gilge, S., Plass-Duelmer, C., Fricke, W., Kaiser, A., Ries, L., Buchmann, B., and Steinbacher, M.: Ozone, carbon monoxide and nitrogen oxides time series at four alpine GAW mountain stations in central Europe, Atmos. Chem. Phys., 10, 12295–12316, doi:10.5194/acp-10-12295-2010, 2010.

Godowitch, J. M., Gilliam, R. C., and Rao, S. T.: Diagnostic evaluation of ozone production and horizontal transport in a regional photochemical air quality modeling system, Atmos. Environ., 45, 3977–3987, 2011.

Gong, W., Dastoor, A. P., Bouchet, V. S., Gong, S., Makar, P. A., Moran, M. D., Pabla, B., Ménard, S., Crevier, L.-P., Cousineau, S., and Venkatesh, S.: Cloud processing of gases and aerosols in a regional air quality model (AURAMS), Atmos. Res., 82, 248–275, 2006.

Graedel, T. E., Bates, T. S., Bouwman, A. F., Cunnold, D., Dignon, J., Fung, I., Jacob, D. J., Lamb, B. K., Logan, J. A., Marland, G., Middleton, P., Pacyna, J. M., Placet, M., and Veldt, C.: A compilation of inventories of emissions to the atmosphere, Global Biogeochem. Cy., 7, 1–26, 1993.

Grell, G. A., Peckham, S. E., Schmitz, R., McKeen, S. A., Frost, G., Skamarock, W. C., and Eder, B.: Fully coupled online chemistry within the WRF model, Atmos. Environ., 39, 6957–6975, 2005.

Guenther, A., Zimmerman, P., and Wildermuth, M.: Natural volatile organic compound emission rate estimates for US woodland landscapes, Atmos. Environ., 28, 1197–1210, 1994.

Guenther, A., Karl, T., Harley, P., Wiedinmyer, C., Palmer, P. I., and Geron, C.: Estimates of global terrestrial isoprene emissions using MEGAN (Model of Emissions of Gases and Aerosols from Nature), Atmos. Chem. Phys., 6, 3181–3210, doi:10.5194/acp-6-3181-2006, 2006.

Hong, S. Y., Noh, Y., and Dudhia, J.: A new vertical diffusion package with an explicit treatment of entrainment processes, Mon. Wea. Rev., 134, 2318–2341, 2006.

Jonson, J. E., Stohl, A., Fiore, A. M., Hess, P., Szopa, S., Wild, O., Zeng, G., Dentener, F. J., Lupu, A., Schultz, M. G., Duncan, B. N., Sudo, K., Wind, P., Schulz, M., Marmer, E., Cuvelier, C., Keating, T., Zuber, A., Valdebenito, A., Dorokhov, V., De Backer, H., Davies, J., Chen, G. H., Johnson, B., Tarasick, D. W., Stübi, R., Newchurch, M.J., von der Gathen, P., Steinbrecht, W., and Claude, H.: A multi-model analysis of vertical ozone profiles, Atmos. Chem. Phys., 10, 5759–5783, doi:10.5194/acp-10-5759-2010, 2010.

Lamarque, J.-F., Bond, T. C., Eyring, V., Granier, C., Heil, A., Klimont, Z., Lee, D., Liousse, C., Mieville, A., Owen, B., Schultz, M. G., Shindell, D., Smith, S. J., Stehfest, E., Van Aardenne, J., Cooper, O. R., Kainuma, M., Mahowald, N., McConnell, J. R., Naik, V., Riahi, K., and van Vuuren, D. P.: Historical (1850–2000) gridded anthropogenic and biomass burning emissions of reactive gases and aerosols: methodology and application, Atmos. Chem. Phys., 10, 7017–7039, doi:10.5194/acp-10-7017-2010, 2010.

Logan, J. A.: An analysis of ozonesonde data for the troposphere: recommendations for testing 3-D models, and development of a gridded climatology for tropospheric ozone, J. Geophys. Res., 104, 115–116, 1999.

Louis, J.: A parametric model of vertical eddy fluxes in the atmosphere, Bound.-La. Meteorol., 17, 197–202, 1979.

Mailhot, J., Bélair, S., Lefaivre, L., Bilodeau, B., Desgagné, M., Girard, C., Glazer, A., Leduc, A.-M., Méthot, A., Patoine, A., Plante, A., Rahill, A., Robinson, T., Talbot, D., Tremblay, A., Vaillancourt, P., Zadra, A., and Qaddouri, A.: The 15-km version of the Canadian regional forecast system, Atmos. Ocean, 44, 133–149, 2006.

Marenco, A., Thouret, V., Nédélec, P., Smit, H., Helten, M., Kley, D., Karcher, F., Simon, P., Law, K., Pyle, J., Poschmann, G., Von Wrede, R., Hume, C., and Cook, T.: Measurement of ozone and water vapor by Airbus in-service aircraft: the MOZAIC airborne program, an overview, J. Geophys. Res., 103, 670–694, 1998.

Matthias, V., Bewersdorff, I., Aulinger, A., and Quante, M.: The contribution of ship emissions to air pollution in the North Sea regions, Environ. Pollut., 158, 2241–2250, 2010.

Matthias, V., Aulinger, A., Bieser, J., Cuesta, J., Geyer, B., Langmann, B., Serikov, I., Mattis, I., Minikin, A., Mona, L., Quante, M., Schumann, U., and Weinzierl, B.: The ash dispersion over Europe during the Eyjafjallajökull eruption – "Comparison of CMAQ simulations to remote sensing and air-borne in-situ observations", Atmos. Environ., 48, 184–194, 2012.

Pepper, D. W., Kern, C. D., and Long, P. E.: Modeling the dispersion of atmospheric pollution using cubic splines and chapeau functions, Atmos. Environ., 13, 223–237, 1979.

Pleim, J. E.: A combined local and nonlocal closure model for the atmospheric boundary layer – Part I: Model description and testing, J. Appl. Meteorol. Clim., 46, 1383–1395, 2007a.

Pleim, J. E.: A combined local and nonlocal closure model for the atmospheric boundary layer – Part II: Application and evaluation in a mesoscale meteorological model, J. Appl. Meteorol. Clim., 46, 1396–1409, 2007b.

Pleim, J. E. and Chang, J. S.: A nonlocal closure-model for vertical mixing in the convective boundary-layer, Atmos. Environ. A, 26, 965–981, 1992.

Pouliot, G., Pierce, T., van der Gon, H. D., Schaap, M., Moran, M., and Nopmongcol, U.: Comparing emission inventories and model-ready emission datasets between Europe and North America for the AQMEII project, Atmos. Environ., 53, 4–14, 2012.

Pudykiewicz, J. A., Kallaur, A., and Smolarkiewicz, P. K.: Semi-Lagrangian modelling of tropospheric ozone, Tellus B, 49, 231–248, 1997.

Rao, S. T., Galmarini, S., and Puckett, K.: Air Quality Model Evaluation International Initiative (AQMEII), B. Am. Meteor. Soc., 92, 23–30, doi:10.1175/2010BAMS3069.1, 2011.

Sartelet, K., Couvidat, F., Seigneur, C., and Roustan, Y.: Impact of biogenic emissions on air quality over Europe and North America, Atmos. Environ., 53, 131–141, 2012.

Schaap, M., Sauter, F., Timmermans, R. M. A., Roemer, M., Velders, G., Beck, J., and Builtjes, P. J. H.: The LOTOS-EUROS model: description, validation and latest developments, Int. J. Environ. Pollut., 32, 270–290, 2008.

Schere, K., Flemming, J., Vautard, R., Chemel, C., Colette, A., Hogrefe, C., Bessagnet, B., Meleux, F., Mathur, R., Roselle, S., Hu, R.-M., Sokhi, R. S., Rao, S. T., and Galmarini, S.: Trace gas/aerosol concentrations and their impacts on continental-scale AQMEII modelling sub-regions, Atmos. Environ., 53, 38–50, 2012.

Simpson, D., Guenther, A., Hewitt, C. N., Steinbrecher, R.: Biogenic emissions in Europe, 1. estimates and uncertainties, J. Geophys. Res., 100, 22875–22890, 1995.

Skamarock, W. C., Klemp, J. B., Dudhia, J., Gill, D. O., Barker, D. M., Duda, M. G., Huang, X. Y., Wang, W., and Powers, J. G.: A Description of the Advanced Research WRF Version 3, NCAR technical note NCAR/TN-475+STR, available at www.mmm.ucar.edu/wrf/users/docs/arw_v3.pdf, June 2008.

Smith, S. J., Pitcher, H., and Wigley, T. M. L.: Global and regional anthropogenic Sulfur Dioxide emissions, Glob. Planet. Change, 29, 99–119, 2001.

Smyth, S. C., Jiang, W., Roth, H., Moran, M. D., Makar, P. A., Yang, F., Bouchet, V. S., and Landry, H.: A comparative performance evaluation of the AURAMS and CMAQ air quality modelling systems, Atmos. Environ., 43, 1059–1070, 2009.

Sofiev, M.: Extended resistance analogy for construction of the vertical diffusion scheme for dispersion models, J. Geophys. Res., 107, 4159, doi:10.1029/2001JD001233, 2002.

Sofiev, M., Galperin, M., and Genikhovich, E.: Construction and evaluation of Eulerian dynamic core for the air quality and emergency modelling system SILAM, in: Air Pollution Modelling and Its Application XIX, NATO Sci. Peace Security Ser. C: Environ. Security, edited by: Borrego, C. and Miranda, A. I., 699–701, Springer, New York, 2008.

Sofiev, M., Genikhovich, E., Keronen, P., and Vesala, T.: Diagnosing the surface layer parameters for dispersion models within the meteorological-to-dispersion modelling interface, J. Appl. Meteorol. Climatol., 49, 221–233, doi:10.1175/2009JAMC2210.1, 2010.

Solazzo, E., Bianconi, R., Vautard, R., Appel, K. W., Moran, M. D., Hogrefe, C., Bessagnet, B., Brandt, J., Christensen, J. H., Chemel, C., Coll, I., van der Gon, H. D., Ferreira, J., Forkel, R., Francis, X. V., Grell, G., Grossi, P., Hansen, A. B., Jericevic, A., Kraljevic, L., Miranda, A. I., Nopmongcol, U., Pirovano, G., Prank, M., Riccio, A., Sartelet, K. N., Schaap, M., Silver, J. D., Sokhi, R. S., Vira, J., Werhahn, J., Wolke, R., Yarwood, G., Zhang, J., Rao, S. T., and Galmarini, S.: Model evaluation and ensemble modelling of surface-level ozone in Europe and North America in the context of AQMEII, Atmos. Environ., 53, 60–74, 2012a.

Solazzo, E., Bianconi, R., Pirovano, G., Matthias, V., Vautard, R., Moran, M. D., Appel, K. W., Bessagnet, B., Brandt, J., Christensen, J. H., Chemel, C., Coll, I., Ferreira, J., Forkel, R., Francis, X. V., Grell, G., Grossi, P., Hansen, A. B., Hogrefe, C., Miranda, A. I., Nopmongco, U., Prank, M., Sartelet, K. N., Schaap, M., Silver, J. D., Sokhi, R. S., Vira, J., Werhahn, J., Wolke, R., Yarwood, G., Zhang, J., Rao, S. T., and Galmarini, S.: Operational model evaluation for particulate matter in Europe and North America in the context of AQMEII, Atmos. Environ., 53, 75–92, 2012b.

Stegehuis, A., Vautard, R., Ciais, P., Teuling, R., Jung, M., and Yiou, P.: Summer temperatures in Europe and land heat fluxes in observation-based data and regional climate model simulations, Clim. Dynam., doi:10.1007/s00382-012-1559-x, online first, 2012.

Stevenson, D. S., Dentener, F. J., Schultz, M. G., Ellingsen, K., van Noije, T. P. C., Wild, O., Zeng, G., Amann, M., Atherton, C. S., Bell, N., Bergmann, D. J., Bey, I., Butler, T., Cofala, J., Collins, W. J., Derwent, R. G., Doherty, R. M., Drevet, J., Eskes, H. J., Fiore, A. M., Gauss, M., Hauglustaine, D. A., Horowitz, L. W., Isaksen, I. S. A., Krol, M. C., Lamarque, J.-F., Lawrence, M. G., Montanaro, V., Müller, J.-F., Pitari, G., Prather, M. J., Pyle, J. A., Rast, S., Rodriguez, J. M., Sanderson, M. G., Savage, N. H., Shindell, D. T., Strahan, S. E., Sudo, K., and Szopa, S.: Multimodel ensemble simulations of present day and near future tropospheric ozone, J. Geophys. Res., 111, D08301, doi:10.1029/2005JD006338, 2006.

Tang, W., Cohan, D. S., Morris, G. A., Byun, D. W., and Luke, W. T.: Influence of vertical mixing uncertainties on ozone simulation in CMAQ, Atmos. Environ., 45, 2898–2909, doi:10.1016/j.atmosenv.2011.01.057, 2011.

Taylor, K. E.: Summarising multiple aspects of model performance in a single diagram, J. Geophys. Res., 106, 7183–7192, 2001.

Thouret, V., Marenco, A., Logan, J. A., Nedelec, P., and Grouhel, C.: Comparison of ozone measurements from the MOZAIC airborne program and the ozone sounding network at eight locations, J. Geophys. Res., 103, 695–720, 1998.

Troen, I. and Mahrt, L.: A simple model of the atmospheric boundary layer: sensitivity to surface evaporation, Bound.-Layer Meteorol., 37, 129–148, 1986.

Van Loon, M., Vautard, R., Schaap, M., Bergström, R., Bessagnet, B., Brandt, J., Builtjes, P. J. H., Christensen, J. H., Cuvelier, C., Graff, A., Jonson, J. E., Krol, M., Langner, J., Roberts, P., Rouil, L., Stern, R., Tarrasón, L., Thunis, P., Vignati, E., White, L., and Wind, P.: Evaluation of long-term ozone simulations from seven regional air quality models and their ensemble average, Atmos. Environ., 41, 2083–2097, 2007.

Vautard, R., Schaap, M., Bergström, R., Bessagnet, B., Brandt, J., Builtjes, P. J. H., Christensen, J. H., Cuvelier, C., Foltescu, V., Graf, A., Kerschbaumer, A., Krol, M., Roberts, P., Rouïl, L., Stern, R., Tarrason, L., Thunis, P., Vignati, E., and Wind, P.: Skill and uncertainty of a regional air quality model ensemble, Atmos. Environ., 43, 4822–4832, 2009.

Vautard, R., Moran, M. D., Solazzo, E., Gilliam, R. C., Matthias, V., Bianconi, R., Chemel, C., Ferreira, J., Geyer, B., Hansen, A. B., Jericevic, A., Prank, M., Segers, A., Silver, J. D., Werhahn, J., Wolke, R., Rao, S. T., and Galmarini, S.: Evaluation of the meteorological forcing used for the Air Quality Model Evaluation International Initiative (AQMEII) air quality simulations, Atmos. Environ., 53, 15–37, 2012.

Vestreng V. and Støren E.: Analysis of the UNECE/EMEP Emission Data, MSC-W Status Report 2000, Norwegian Meteorological Institute: Blindern, Oslo, 2000.

Walcek, C. J.: Minor flux adjustment near mixing ratio extremes for simplified yet highly accurate monotonic calculation of tracer advection, J. Geophys. Res., 105, 9335–9348, 2000.

Yarwood, G., Rao, S., Yocke, M., and Whitten, G.: Updates to the Carbon Bond Chemical Mechanism: CB05, US EPA report RT-0400675, available at: http://www.camx.com (last access: 9 November 2012), 2005.

Yu, S. C., Mathur, R., Kang, D., Schere, K., Pleim, J., and Otte, T. L.: A detailed evaluation of the Eta-CMAQ forecast model performance for O_3, its related precursors, and meteorological parameters during the 2004 ICARTT study, J. Geophys. Res., 112, D12S14, doi:10.1029/2006JD007715, 2007.

Yu, S., Mathur, R., Sarwar, G., Kang, D., Tong, D., Pouliot, G., and Pleim, J.: Eta-CMAQ air quality forecasts for O_3 and related species using three different photochemical mechanisms

(CB4, CB05, SAPRC-99): comparisons with measurements during the 2004 ICARTT study, Atmos. Chem. Phys., 10, 3001–3025, doi:10.5194/acp-10-3001-2010, 2010.

Zhang, J. and Rao, S. T.: The role of vertical mixing in the temporal evolution of ground-level ozone concentrations, J. Appl. Meteorol., 38, 1674–1691, 1999.

Zyryanov, D., Foret, G., Eremenko, M., Beekmann, M., Cammas, J.-P., D'Isidoro, M., Elbern, H., Flemming, J., Friese, E., Kioutsioutkis, I., Maurizi, A., Melas, D., Meleux, F., Menut, L., Moinat, P., Peuch, V.-H., Poupkou, A., Razinger, M., Schultz, M., Stein, O., Suttie, A. M., Valdebenito, A., Zerefos, C., Dufour, G., Bergametti, G., and Flaud, J.-M.: 3-D evaluation of tropospheric ozone simulations by an ensemble of regional Chemistry Transport Model, Atmos. Chem. Phys., 12, 3219–3240, doi:10.5194/acp-12-3219-2012, 2012.

Title Page
Abstract Introduction
Conclusions References
Tables Figures
◀| |▶
◀ ▶
Back Close
Full Screen / Esc
Printer-friendly Version
Interactive Discussion

Table 1. Airport domains and number of hourly flights for 2006. for each field. The airports selected for analyses are highlighted in bold.

Domain	Airports	IATA Code	Num. of Avail. flights	O_3	CO	T	RH	WS	WD
West Cast	**Portland**	KPDX	142	126	135	142	142	142	142
	Vancouver	CYVR	72	62	65	72	72	72	72
Atlanta	**Atlanta**	KATL	142	126	129	142	141	142	142
	Charlotte	KCLT	2	2	2	2	2	2	2
East Coast	Boston	KBOS	30	27	26	30	30	30	30
	Chicago	KORD	4	4	4	4	4	4	4
	Montreal	CYUL	2	2	2	2	2	2	2
	New York	KJFK	15	10	15	15	15	15	15
	Philadelphia	KPHL	110	102	102	109	109	110	110
	Toronto	CYYZ	90	72	72	89	89	89	89
	Washington	KIAD	62	28	54	61	61	62	62
Dallas	**Dallas**	KDFW	124	124	114	121	124	124	124
Central Europe	**Frankfurt**	EDDF	1214	1088	1134	1134	1135	1135	1026
	München	EDDM	6	4	6	6	6	6	6
	Vienna	LOWW	374	291	374	360	374	374	249

Table 2. Participating models and features.

Met	CTM	Resolution (km)	Vertical (bottom-top)	Emission	BC
			North America		
GEM	AURAMS	15 × 15	28 (14 in the first 2 km)	Standard[b]	Climatology
MM5	DEHM	50 × 50	29 (100 hPa)	Global emission database/EMEP[d]	Estimated from hemispheric domain
WRF	CMAQ	12 × 12	34 (25 m to 50 hPa)	Standard	Standard
WRF	CAMx	12	23 from 30 m	Standard	standard
Cosmo-CLM (CCLM)	CMAQ	24 × 24	30 (60 m to 100 hPa)	Standard[a]	Standard
			Europe		
MM5	DEHM	50 × 50	29 (100 hPa)	Global emission database/EMEP[d]	Estimated from hemispheric domain
ECMWF	SILAM	24	9 (10 km)	Standard	Standard
MM5	CHIMERE	25	9 (20 m to 500 hPa)	Standard	Standard, MEGAN
ECMWF	LOTOS-EUROS	25	4	Standard[a]	Standard
WRF	CMAQ	18	34	Standard[a]	Standard
MM5	CAMx	15	26 from 40 m	Standard	Standard
WRF	WRF-Chem	22.5	36	Standard[a]	Standard
Cosmo-CLM (CCLM)	CMAQ	24 × 24	30 (36 m to 100 hPa)	Standard[a]	Standard
WRF	WRF-Chem	22.5	36	Standard[a]	Standard
MM5	Polyphemus	24	9 (up to 1200 m)	Standard[a,c]	Standard

[a] Standard anthropogenic emission and biogenic emission derived from meteorology (temperature and solar radiation) and land use distribution implemented in the meteorological driver (Guenther et al., 1994; Simpson et al., 1995).

[b] Standard anthropogenic inventory but independent emissions processing, exclusion of wildfires, and different version of BEIS (v3.09) used.

[c] Emissions Includes: Biomass burning; Biogenic organic compounds of SOA:a-pinene, limonene, sesquiterpene, hydrophilic isoprene.

[d] Global: IPCC RCP 3-PD Lamarque et al. (2010); Bond et al. (2007); Smith et al. (2001); Ships: Corbett and Fischbeck (1997); GEIA natural emissions (Graedel et al., 1993); Wildfires as in Schultz et al. (2008). Europe: EMEP (Vestreng and Støren, 2000).

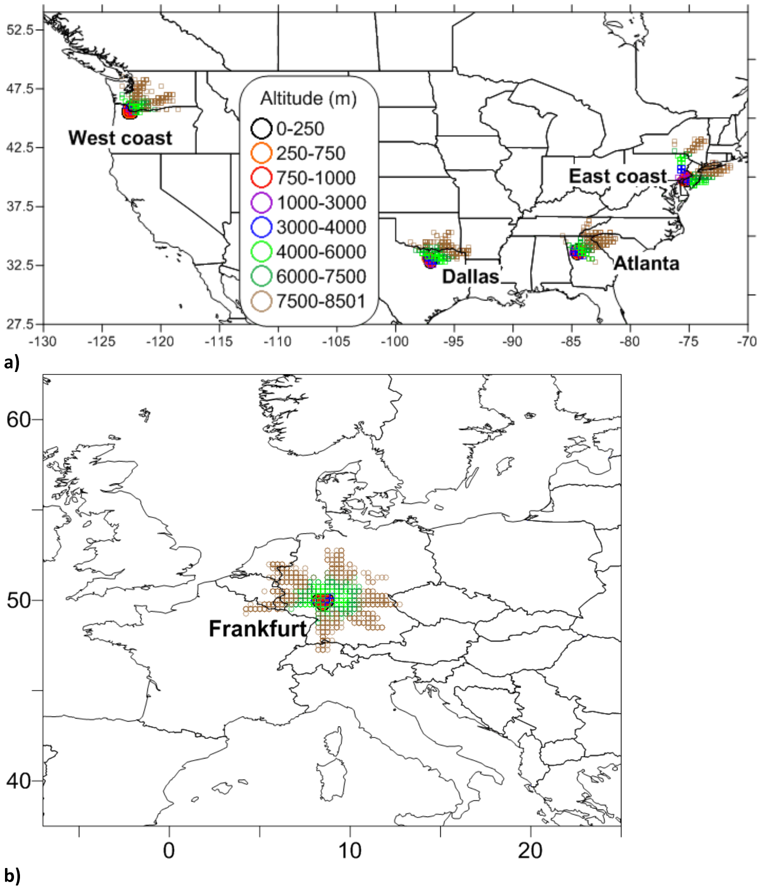

Fig. 1. Flight trajectories by height for the selected airports of **(a)** North America and **(b)** Europe.

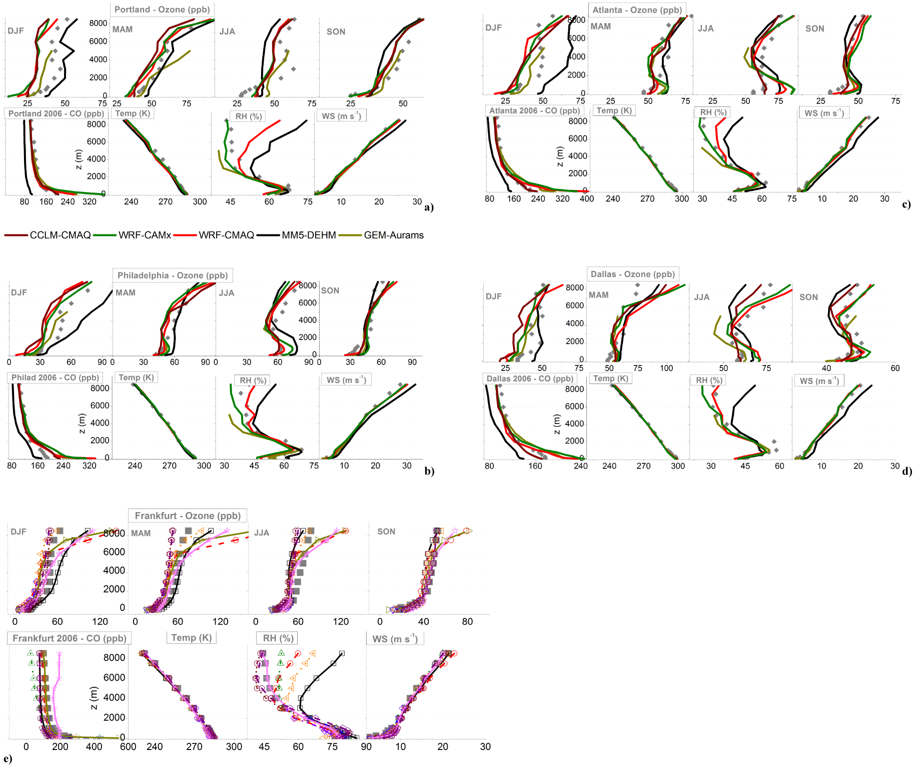

Fig. 2. Seasonal averaged mean profiles of ozone (top panels) and annual averaged mean profiles of CO, temperature, relative humidity and wind speed (lower panels) for **(a)** Portland, **(b)** Philadelphia, **(c)** Atlanta, **(d)** Dallas, and **(e)** Frankfurt. The symbols in gray are the observations.

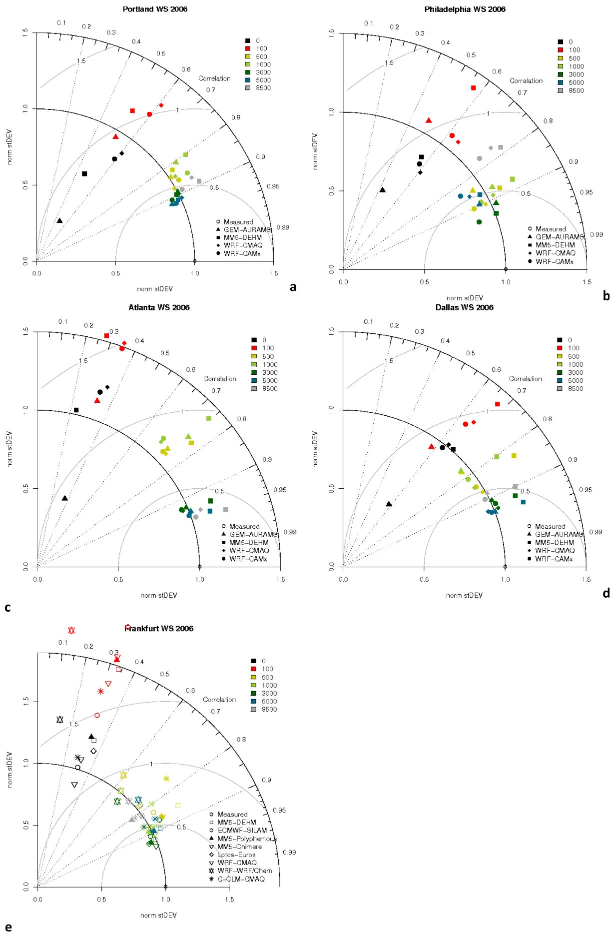

Fig. 3. Taylor diagrams for wind speed at **(a)** Portland; **(b)** Philadelphia; **(c)** Atlanta; **(d)** Dallas; **(e)** Frankfurt.

GMDD

6, 521–584, 2013

Four-dimensional evaluation of regional air quality models

E. Solazzo et al.

Title Page
Abstract Introduction
Conclusions References
Tables Figures
◀| |▶
◀ ▶
Back Close
Full Screen / Esc
Printer-friendly Version
Interactive Discussion

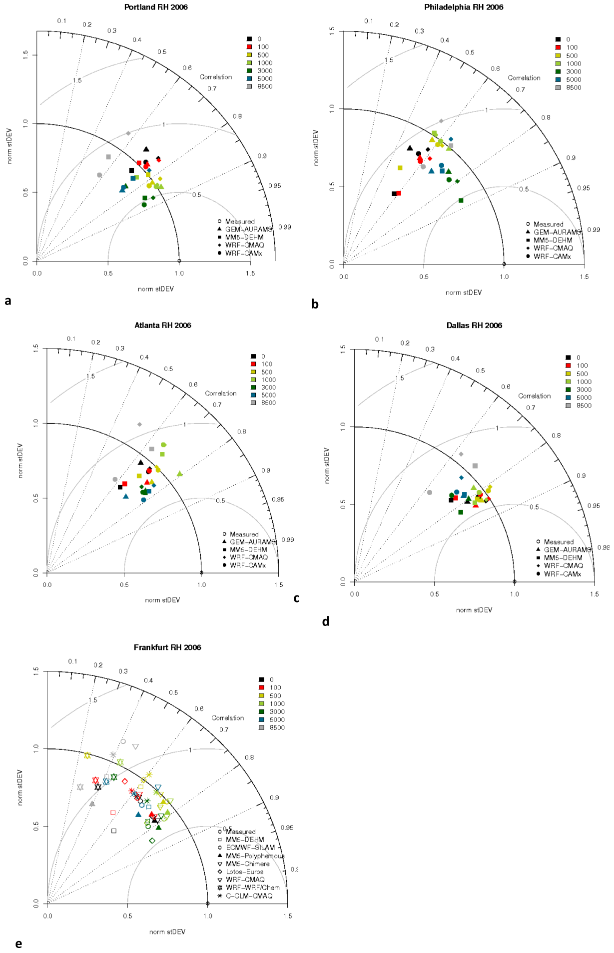

Fig. 4. Taylor diagrams for relative humidity at **(a)** Portland; **(b)** Philadelphia; **(c)** Atlanta; **(d)** Dallas; **(e)** Frankfurt. Height by colors, model by symbols.

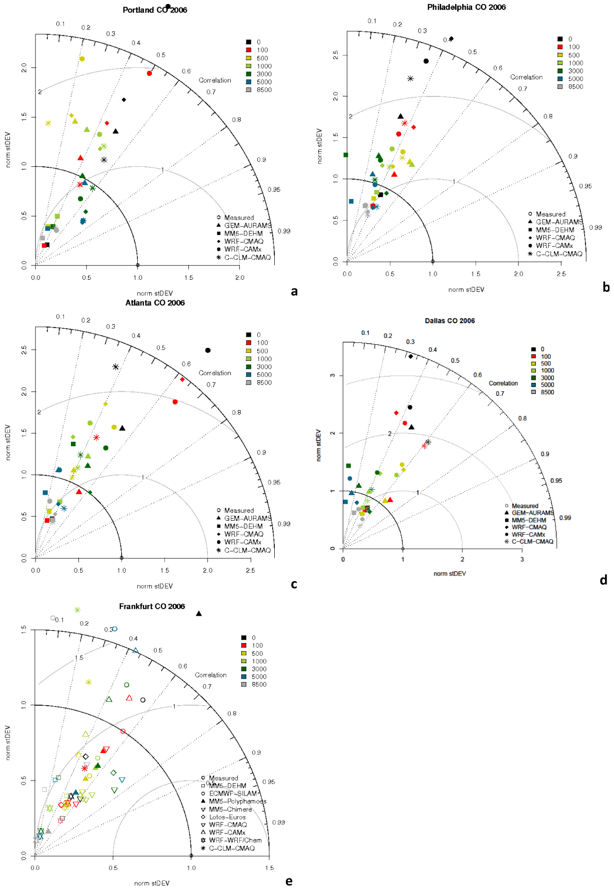

Fig. 5. Taylor diagrams for CO at **(a)** Portland; **(b)** Philadelphia; **(c)** Atlanta; **(d)** Dallas; **(e)** Frankfurt. Height by colors, model by symbols.

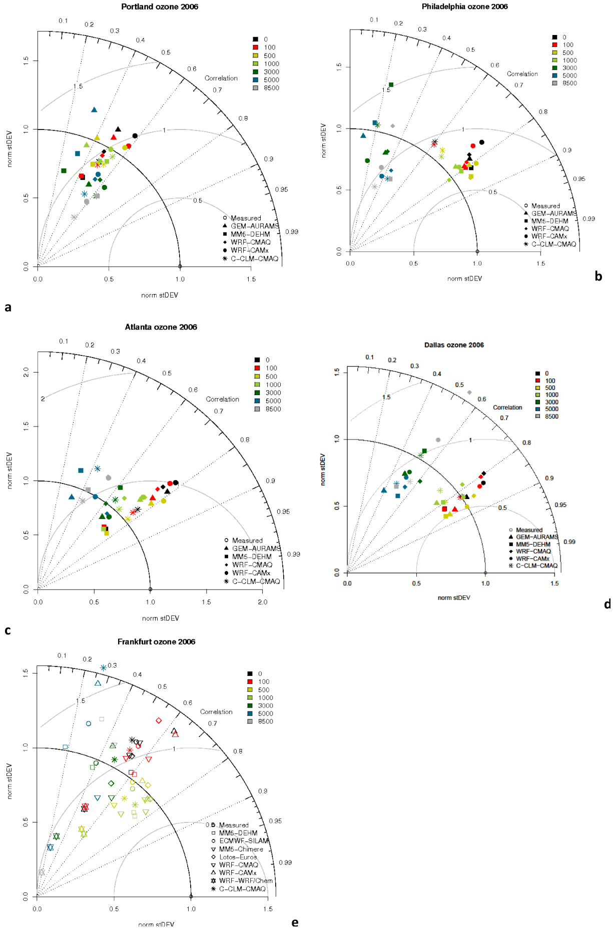

Fig. 6. Taylor diagrams for ozone at **(a)** Portland; **(b)** Philadelphia; **(c)** Atlanta; **(d)** Dallas; **(e)** Frankfurt. Height by colors, model by symbols.

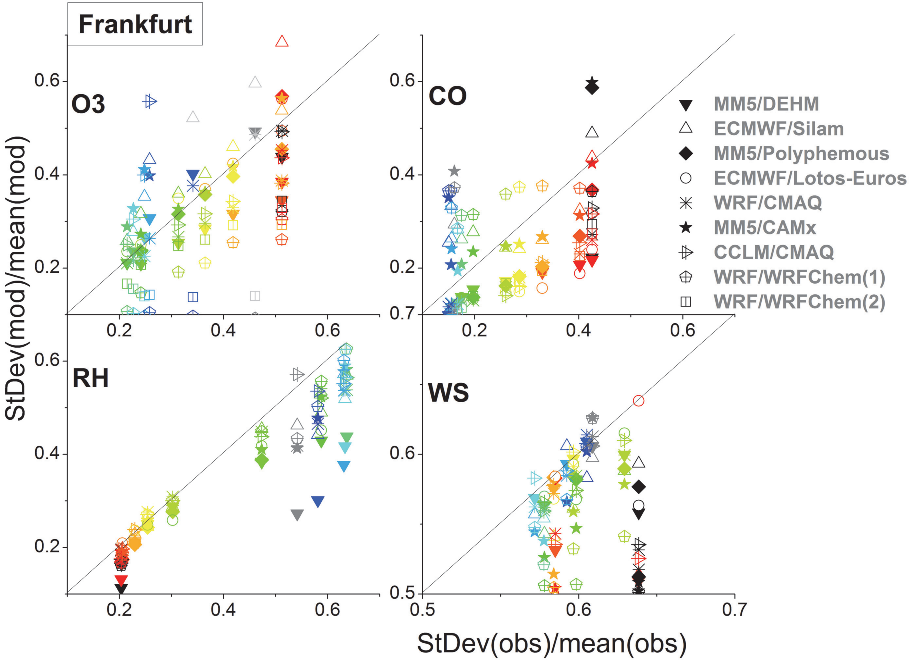

Fig. 7. Coefficient of variation for Frankfurt. Clockwise from top left panel: ozone, CO, wind speed, relative humidity.

Title Page
Abstract
Introduction
Conclusions
References
Tables
Figures
◀▮
▶▮
◀
▶
Back
Close
Full Screen / Esc
Printer-friendly Version
Interactive Discussion

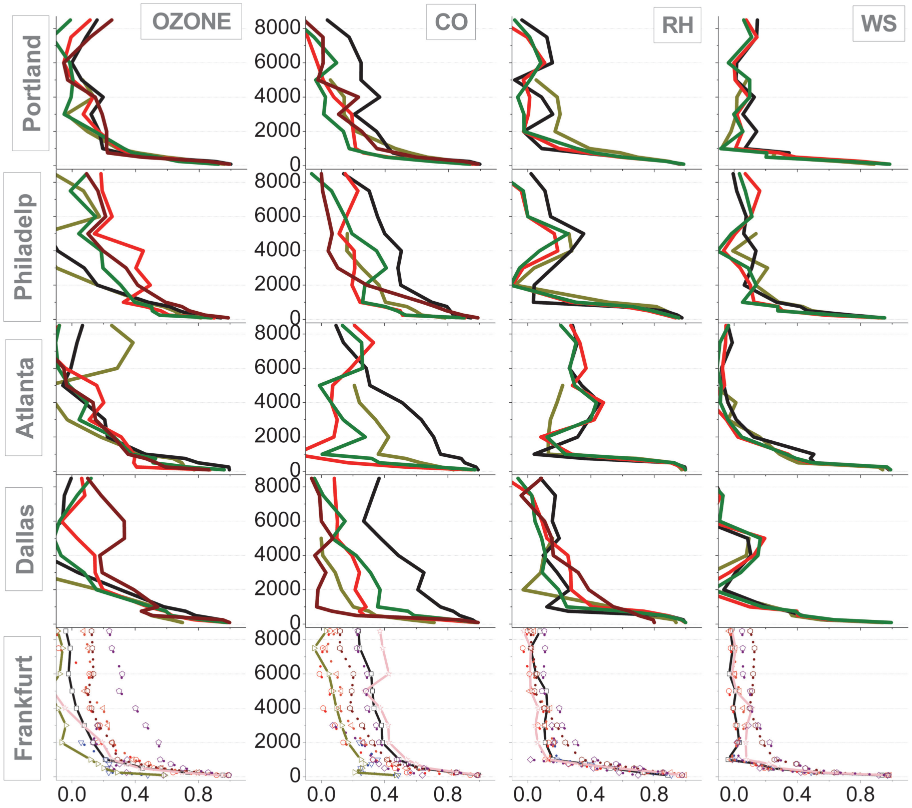

Fig. 8. Correlation coefficient between the FD at any height and the FD at the ground ($z = 0$) for ozone, CO, RH, and WS (columns) and for the airports of Portland, Philadelphia, Atlanta, Dallas, and Frankfurt (rows) (year 2006). Legend as in Fig. 2.

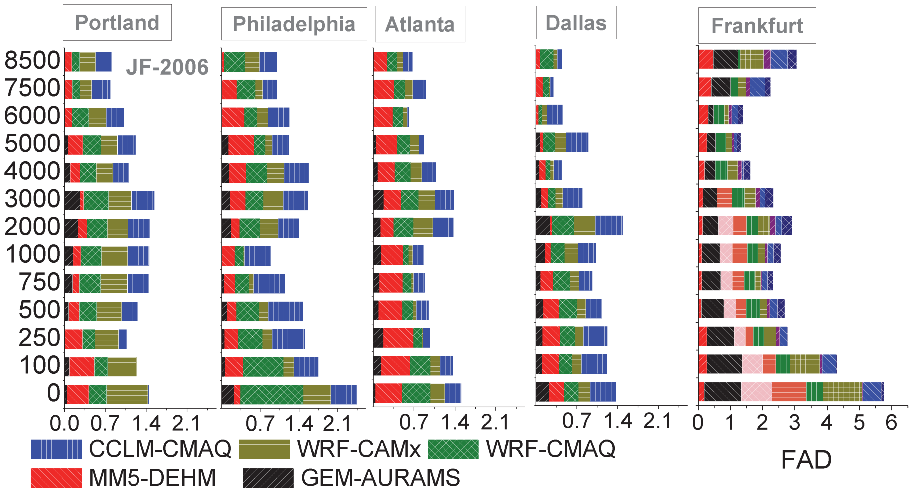

Fig. 9. Cumulative Fractional Absolute Difference (FAD) of modelled ozone over the months of January and February 2006. The legend refers to the North American's airports. Legend for Frankfurt in the next figure.

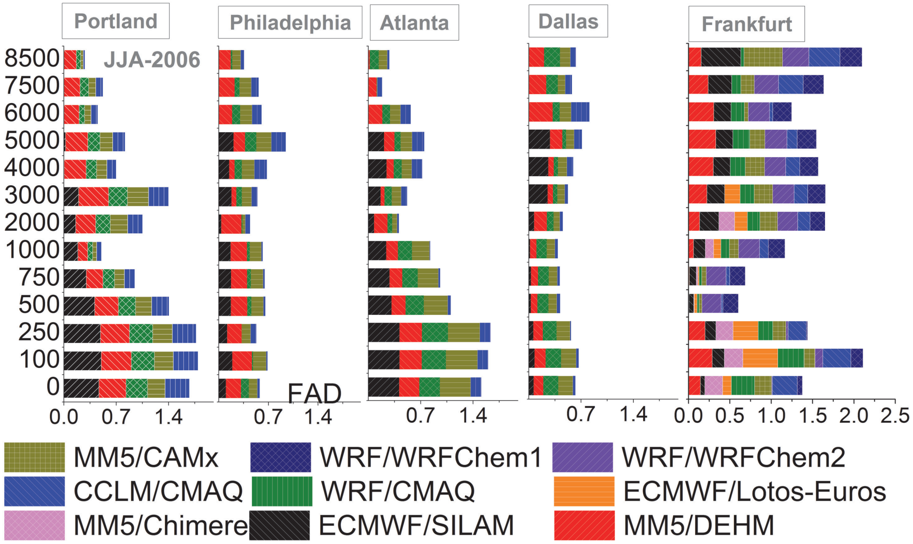

Fig. 10. Cumulative Fractional Absolute Difference (FAD) of modelled ozone over the months of June-July-August 2006. The legend refers to Frankfurt only. Legend for North American's airports in the previous figure.

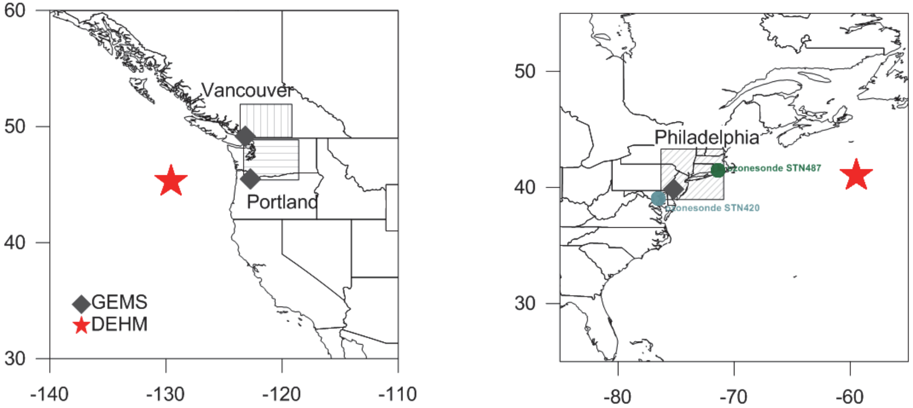

Fig. 11. Positions of nodes where BCs data are provided for GEMS and DEHM (AURAMS node is the same as the GEMS). For the East Coast the locations of two ozonesondes used in the analysis are also shown.

Title Page
Abstract | Introduction
Conclusions | References
Tables | Figures
◀| |▶
◀ ▶
Back | Close
Full Screen / Esc
Printer-friendly Version
Interactive Discussion

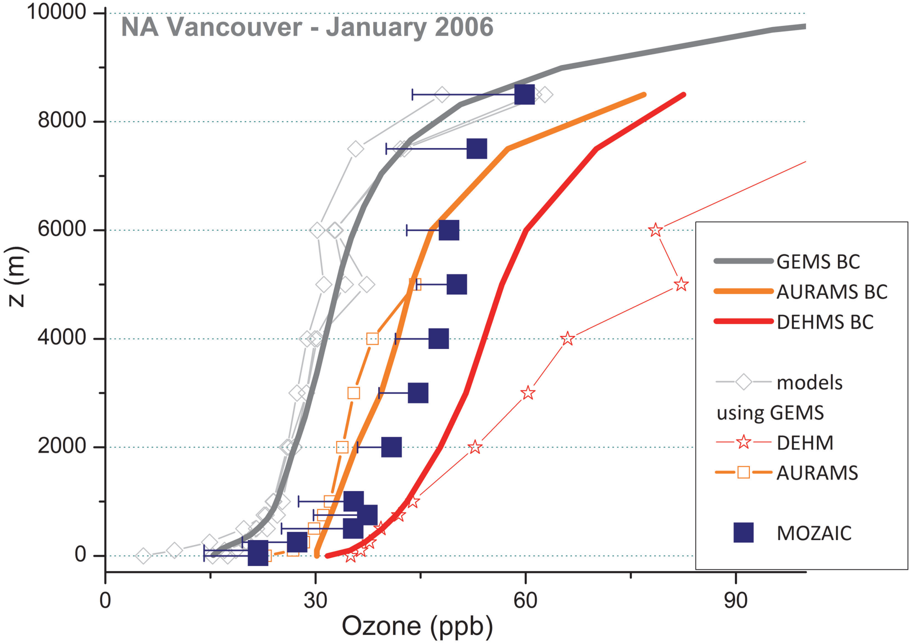

Fig. 12. Monthly averaged vertical profiles of ozone for Vancouver, January 2006: BC providers (thick lines), AQ model outputs (thin lines), MOZAIC (filled squares). The horizontal lines by the measurements are the standard deviations (symmetric about the mean point, thus only the left portion is shown).

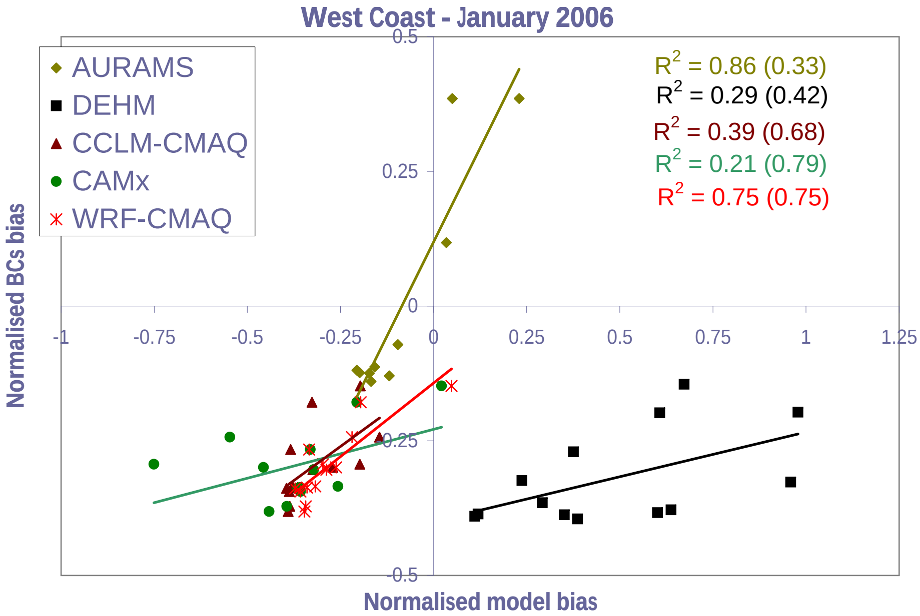

Fig. 13. Normalised modelled vs. BCs bias with respect to MOZAIC for the month of January 2006 over the Portland airport. The two CMAQ instances and CAMx use the same BCs. The continuous lines derive from the linear regression fit, with the squared correlation coefficients reported on the top right corner (color coded). In parenthesis are the squared coefficients obtained by correlating the bias excluding the data in the first 250 m (i.e. from 500 m to 8500 m).

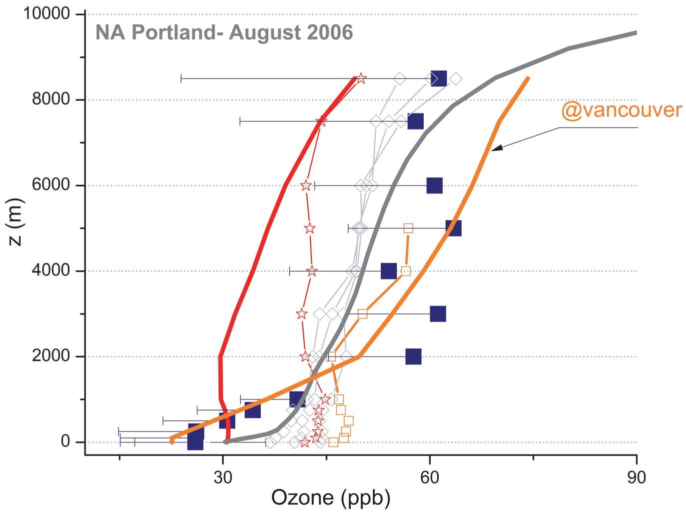

Fig. 14. Monthly averaged vertical profiles of ozone for Portland, August 2006. Legend as in Fig. 12. The BC for the AURAMS model (thick orange line) was provided at Vancouver.

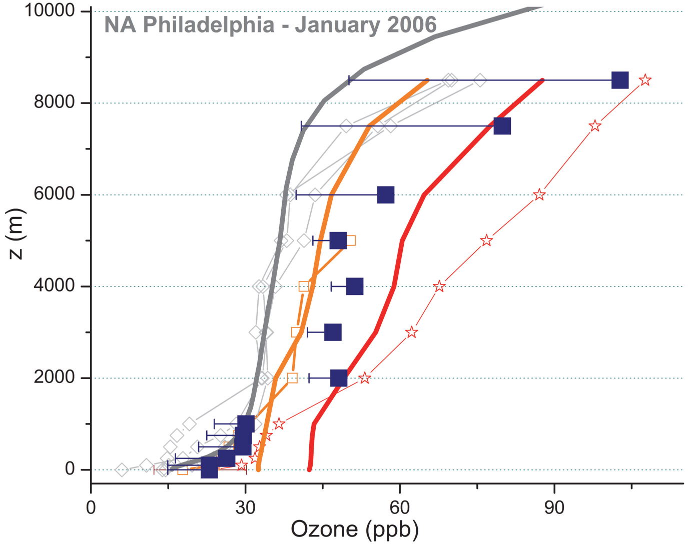

Fig. 15. Monthly averaged vertical profiles of ozone for Philadelphia, January 2006. Legend as in Fig. 12.

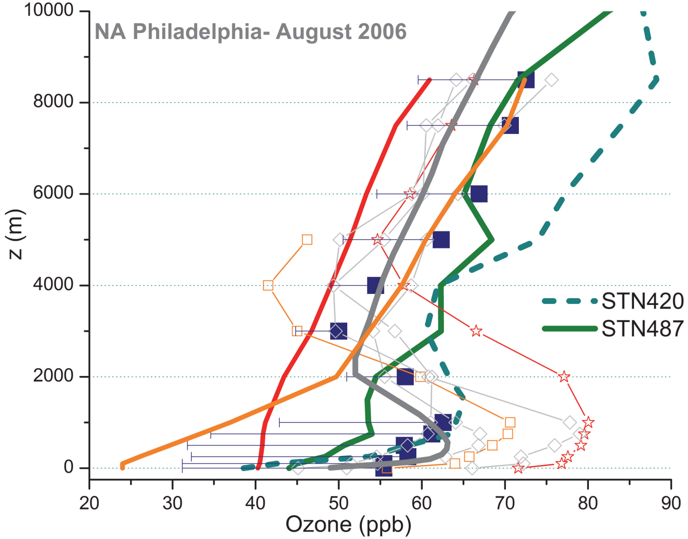

Fig. 16. Monthly averaged vertical profiles of ozone for Philadelphia, August 2006. Legend as in 12. Monthly averaged ozonesonde profiles from two nearby rural locations are also reported.